International Journal of Computer Vision 32(3), 195–212 (1999)

Geometry of Distorted Visual Space and Cremona Transformation

LOONG-FAH CHEONG
Electrical Engineering Department, National University of Singapore, 10 Kent Ridge Crescent, Singapore 119260

KOK-ONN NG
Mathematics Department, National University of Singapore, 10 Kent Ridge Crescent, Singapore 119260

Received January 22, 1998; Revised October 23, 1998; Accepted October 29, 1998

Abstract. An important issue concerning the design of any vision system is the choice of a proper space representation. In order to search for clues to a suitable representation, we look at the distortion of space arising from errors in motion or stereo estimates. Understanding this space distortion has important epistemological implications for the problem of space representation because it tells us what can be and what cannot be computed. This paper is therefore an enquiry into the nature of space representation through the study of the space distortion, though it is not a psychophysical or physiological study but rather a computational one. We show that the distortion transformation is a quadratic Cremona transformation, which is bijective almost everywhere except on the set of fundamental elements. We identify the fundamental elements of both the direct and the inverse transformations, and study the behaviour of the space distortion by analyzing the transformation of space elements (lines, planes) that pass through these fundamental elements.

Keywords: motion analysis, structure from motion, stereopsis, error analysis, shape representation, cremona transformation

1. Introduction

An important issue concerning the design of any vision system is the choice of a proper space representation. This representation of space must allow us to abstract essential information in a real-time manner. The classical reconstruction theory, as articulated by Marr (1982), attempts to recover a metric representation of space which is general-purpose and thus can be used for any task. Despite more than a decade of efforts, we still lack robust and real-time algorithms to extract such a 3D space representation. This state of affairs has led to a re-evaluation as to what constitutes an appropriate space representation.

In recent years, there emerged the paradigm of Active Vision or Purposive Vision, which emphasizes visual recovery as part of a perception-action cycle, as opposed to something in isolation (Aloimonos et al., 1988). Recovery of shape and orientation information in the general case is eschewed; the emphasis is on what should be done with computations in vision. Such representations include a limited amount of information, as required by a particular task. The assumption is that the computation of concise representations requires less information and fewer assumptions, and may be therefore potentially more robust.

The results in this paper suggest that restricting the information recovered from images alone does not guarantee that it is more reliable. The form of the space representation is also innately constrained by what could be computed. It is at the level of inherent constraints upon which we wish to focus our enquiry. The elucidation of these inherent constraints, and of how certain aspects of the 3D scene may be more sensitive to perturbations than others would eventually pave the way for deriving an appropriate space representation.

Different visual cues might give rise to different forms of space representations. Each cue may represent

a different, partial aspect of the physical space around the observer. This paper focuses upon the perception of space arising from motion and stereo cues, though the concept proposed has general applicability. Of the two cues, stereo can be treated as a special case of motion. Thus most of our discussions and analyses will be dealing with the general case of motion.

Motion and stereo are among the most important visual cues used for space perception. In spite of the often complex mathematical treatment that they receive, they are perhaps the most intuitive to understand, and at the same time capable of elegant geometrical characterization. Yet, robust depth estimates have been difficult to obtain. Due to inaccuracies in the way motion is perceived, or in the way parameters of the stereo apparatus are estimated, the recovered structure from motion and to a lesser extent from stereo invariably contains systematic distortion.

A proper representation of space cannot be obtained unless one tackles the interaction between the errors in motion or stereo estimates and the corresponding distortion in depth. Understanding the nature of the space distortion would have important epistemological implications for the problem of space representation because it tells us what can be and what cannot be computed. The fundamental contribution of this paper is the development of a computational framework showing the geometric laws under which the recovered scene is distorted. The systematic way in which visual space is distorted is therefore made explicit; we show that the transformation from physical to perceptual space belongs to the family of Cremona transformations (Hudson, 1927; Semple and Roth, 1949), which is bijective almost everywhere except on the set of fundamental elements.

The power of the computational framework introduced was demonstrated in two companion articles (Cheong et al., 1998; Fermüller et al., 1997). First, the framework has allowed us to present a number of geometric arguments regarding the inherent ambiguity in image sequences as far as 3D motion estimation is concerned (Cheong et al., 1998). It has also been used to explain the psychophysics of the distortion of visual space experienced by human observers from stereo or motion (Fermüller et al., 1997). In this paper, we focus on developing mathematical results on the shape distortion transformation. Specifically, we identify the fundamental elements of the direct and the inverse transformations, and study the behaviour of the space distortion by analyzing the transformation of space elements (lines, planes) that pass through these fundamental elements.

2. Literature Review

2.1. Estimation of 3D Motion and Structure

Motion is one of the most important cues that gives rise to space perception and has therefore attracted considerable research in the past decade (Fermüller, 1995; Heeger and Jepson, 1992; Heel, 1990; Horn, 1987; Longuet-Higgins, 1981; Maybank, 1993; Spetsakis and Aloimonos, 1988; Tsai and Huang, 1984; Uras et al., 1988; Weng et al., 1991). Its computational aspects have been studied extensively as two subproblems, namely, the measurement of 2D image velocity (also called optical flow), and the extraction of 3D scene structure and egomotion from the image velocity measurements. These studies have given rise to several algorithms for deriving the 3D structure and motion. Experimentation with these algorithms, however, has revealed the lack of robustness in practice. A small amount of error in the image measurements can lead to very different solutions (Barron et al., 1987; Dutta and Snyder, 1990; Tsai and Huang, 1984; Weng et al., 1991).

The ill-conditioned nature of the computation has since then prompted many analyses. One problem is due to the inherent ambiguity in determining the motion (Horn, 1987; Krames, 1940; Maybank, 1993; Negahdaripour, 1987, 1989), that is, different motion/surface pairs (not related through a scaling factor) can give rise to mathematically identical motion fields. It has been shown that the ambiguity is only possible if the scene in view lies on certain hyperboloids of one sheet, or their degeneracies, the so-called critical surfaces. In practice, it is rare to encounter configurations that are exactly ambiguous. Nevertheless, when the image velocity measurements or the image correspondences contain noise, the instability in reconstruction and the ambiguity are not unrelated: Maybank (1993) showed that a small perturbation can be found such that the resulting set of image correspondences or image velocities becomes ambiguous.

Compounding the aforementioned problem is the difficulty in computing feature correspondences or optical flow vectors. The difficulty arises as a consequence of the aperture problem. The need to combine local motion constraints over an area of the image, or along contours, often leads to errors in the optical

flow, not to mention its considerable computational requirement. Several techniques have been proposed to address this problem, examples of which are robust statistics (Black, 1994; Bober and Kittler, 1994), higher order flow constraints (Uras et al., 1988), constraint line clustering (Schunck, 1989), and the phase-based approach (Fleet, 1992). Each has different advantages and shortcomings in terms of accuracy, computational efficiency and measurement density. In practice, several aspects of the image formation process contribute further uncertainty. For instance, Verri and Poggio (1989) showed that the 2D motion field (the projection on the image plane of the 3D velocity field) and the optical flow vectors are in general quantitatively different, unless very special conditions are satisfied.

In view of such errors, several analyses relate the errors of the estimated motion parameters in the second step to the measurement errors in the first step. The errors are typically expressed as a high variance or a bias in the motion parameters through some statistical analysis (Adiv, 1989; Daniilidis and Nagel, 1993; Duric and Aloimonos, 1994; Thomas et al., 1993; Weng et al., 1991; Young and Chellapa, 1992), or given as empirical figures through some simulations (Barron et al., 1987; Dutta and Snyder, 1990). A comprehensive survey of such analysis is given by Daniilidis and Spetsakis (1997). Based on a combination of qualitative analysis and quantitative simulations, the following observations regarding reliable motion estimation can be made:

- The field of view should be large in order to obtain more reliable motion estimates. If field of view is small or depth variation is insufficient, rotations about an axis parallel to the image plane can easily be confounded with lateral translations.
- The magnitude of translational flow should be large relative to rotational flow in order to obtain reliable translational direction and accurate structure of the scene. Thus either the scene should be near or the translational motion should be large.
- In the case of a small field of view, the estimated translation is biased towards the viewing direction if the error metric is not appropriately normalized.

2.2. Errors in Depth Estimation

While the various analyses discussed in the preceding paragraphs have advanced our understanding of the errors in the motion parameters and the circumstances that give rise to them, the corresponding issues on the errors in depth estimation is much less explored. Due to the complexity of the problem, most of the analyses on the errors in the depth estimates are of an empirical nature, dealing with specific motions or scene types (Adiv, 1989; Dutta and Snyder, 1990). For instance, the translation involved was restricted to forward motion only, or the scene in view consisted of a planar surface. It is being understood that small errors in the motion estimates can lead to very large errors in the depth estimates (Dutta and Snyder, 1990). Notably absent in all these analyses is an account of the systematic errors of the depth estimates that result from erroneous motion estimates. While Thomas et al. (1993) represent such systematic distortion using an error covariance matrix, the matrix formulation is motivated by the need to represent structure errors in a recursive estimation algorithm. Therefore the geometric mapping involved in the distortion is not made explicit. Due to the lack of such an analysis, the relationship between the distorted surfaces and the true surfaces for arbitrary motion errors is not well understood, except in the case of critical surface pairs (Horn, 1987; Krames, 1940; Negahdaripour, 1987, 1989), where the relationship is explicitly stated.

2.3. Human's Depth Perception from Motion and Stereopsis

In the field of psychophysics, there is strong evidence that the perceived visual space and the physical space are not similar (Foley, 1967, 1980; Johnston, 1991; Ogle, 1964; Tittle et al., 1995). Many psychophysical experiments report that while our perceptual judgments can be quite accurate in some instances, other aspects of the perceived visual space are systematically distorted. In an effort to develop an explanation for the relationship between the physical and the perceived space, the general approach among the psychophysical community has been based on the hierarchy of geometries proposed by Felix Klein in his *Erlangen Program*. The idea is that any geometric transformation will alter some of the structural properties of the scene while leaving others invariant. If one considers the mapping between physical and perceived space as a geometric transformations, then it follows from Klein's analysis that some properties of 3D structure will be systematically distorted and others will remain invariant. This has led to a series of investigations that analyze the specific perceptual tasks that yield accurate or inaccurate performance, so that the geometric transformations between the physical and perceived space can be

identified. Some of the candidate transformations are Euclidean, similarity, affine, or Riemannian, among others. Nevertheless, much of the results seem to suggest that the transformation is more complex than can be easily accounted for by one of these transformations. For instance, the expansion of depth at near distances and the contraction of depth at far distances has been reported by numerous investigators (Foley, 1980; Johnston, 1991; Tittle et al., 1995), which is inconsistent with what is expected if the mapping between physical and perceived space were affine. In contrast to a synthetic approach, the iso-distortion framework proposed in this paper offers an analytic account of several properties of the perceived visual space. Our analysis shows that the transformation between physical and perceptual space is more complicated than previously thought.

The paper is organized as follows. Section 3 develops the equations leading to the iso-distortion framework. Section 4 shows that the transformation from physical to perceptual space belongs to the family of Cremona transformations, and applies some established results from the mathematical literature on Cremona transformation to the shape distortion transformation. Sections 5 and 6 relate the iso-distortion surfaces to Cremona transformation. The paper ends with a short description of future work and conclusions.

3. Distortion of Visual Space

As an image formation model, we use the standard model of perspective projection on the plane, with the image plane at a distance f from the nodal point parallel to the XY plane, and the viewing direction along the positive Z-axis as illustrated in Fig. 1.

The change of viewing geometry is described through a rigid motion with translational velocity (U, V, W) and rotational velocity (α, β, γ) of the observer in the coordinate system $OXYZ$ (see Fig. 1).

As a consequence of the scaling ambiguity, only the direction of translation $(x_0, y_0) = (\frac{U}{W} f, \frac{V}{W} f)$ represented in the image plane by the epipole (also called the FOE (focus of expansion) or FOC (focus of contraction) depending on whether W is positive or negative), the scaled depth Z/W and the rotational parameters can possibly be obtained from flow measurements. Using this notation the equations relating the 2D velocity $\mathbf{u} = (u, v) = (u_{\text{trans}} + u_{\text{rot}}, v_{\text{trans}} + v_{\text{rot}})$ of an image point to the 3D velocity and the depth of the corresponding scene point are (Longuet-Higgins, 1981)

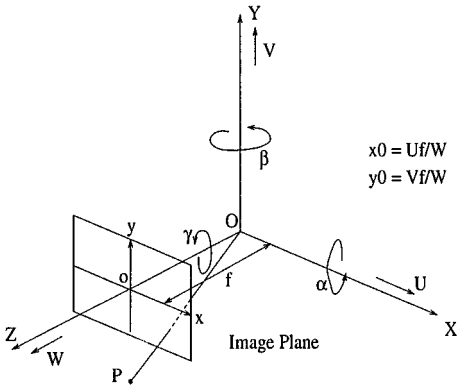

Figure 1. The image formation model. $OXYZ$ is a coordinate system fixed to the camera. O is the optical center and the positive Z-axis is the direction of view. The image plane is located at a focal length f pixels from O along the Z-axis. A point P at (X, Y, Z) in the world produces an image point p at (x, y) on the image plane where (x, y) is given by $(\frac{fX}{Z}, \frac{fY}{Z})$. The instantaneous motion of the camera is given by the translational vector (U, V, W) and the rotational vector (α, β, γ).

$$
\begin{aligned}
u &= u_{\text{trans}} + u_{\text{rot}} \\
&= (x - x_0)\frac{W}{Z} + \frac{\alpha xy}{f} - \beta\left(\frac{x^2}{f} + f\right) + \gamma y \\
v &= v_{\text{trans}} + v_{\text{rot}} \\
&= (y - y_0)\frac{W}{Z} + \alpha\left(\frac{y^2}{f} + f\right) - \frac{\beta xy}{f} - \gamma x
\end{aligned} \tag{1}
$$

where $u_{\text{trans}}, v_{\text{trans}}$ are the horizontal and vertical components of the flow due to translation, and $u_{\text{rot}}, v_{\text{rot}}$ the horizontal and vertical components of the flow due to rotation, respectively.

The normal flow $\mathbf{u}_n$ measured along a direction $\mathbf{n} = (n_x, n_y)$ normal to the intensity gradient is given by

$$u_n = un_x + vn_y. \tag{2}$$

Knowing the parameters of the viewing geometry exactly, the scaled depth can be derived from (2). Since the depth can only be derived up to a scale factor, we set $W = 1$ and obtain

$$Z = \frac{(x - x_0)n_x + (y - y_0)n_y}{u_n - u_{\text{rot}}n_x - v_{\text{rot}}n_y}$$

If there is an error in the estimation of the viewing geometry, this will in turn cause errors in the estimation of the scaled depth, and thus a distorted version of space will be computed. To distinguish between the various estimates, we use the hat sign " ˆ " to represent estimated quantities, the unmarked letters to denote the actual quantities, and the subscript "ϵ" to represent errors, where the estimates are related as follows:

$$
\begin{aligned}
(\hat{x}_0, \hat{y}_0) &= \left(x_0 - x_{0_\epsilon}, y_0 - y_{0_\epsilon}\right) \\
(\hat{\alpha}, \hat{\beta}, \hat{\gamma}) &= (\alpha - \alpha_\epsilon, \beta - \beta_\epsilon, \gamma - \gamma_\epsilon) \\
\hat{\mathbf{u}}_{\text{rot}} &= \left(u_{\text{rot}} - u_{\text{rot}_\epsilon}, v_{\text{rot}} - v_{\text{rot}_\epsilon}\right) \\
&= \left[u_{\text{rot}} - \left(\frac{\alpha_\epsilon xy}{f} - \beta_\epsilon\left(\frac{x^2}{f} + f\right) + \gamma_\epsilon y\right),\right. \\
&\qquad \left. v_{\text{rot}} - \left(\alpha_\epsilon\left(\frac{y^2}{f} + f\right) - \beta_\epsilon \frac{xy}{f} - \gamma_\epsilon x\right)\right]
\end{aligned}
$$

If we also allow for a noise term N in the estimate $\hat{u}_n$ of the component flow u_n, we have $\hat{u}_n = u_n - N$. The estimated depth becomes

$$
\hat{Z} = \frac{(x - \hat{x}_0)\, n_x + (y - \hat{y}_0)\, n_y}{\hat{u}_n - (\hat{u}_{\text{rot}} n_x + \hat{v}_{\text{rot}} n_y)} \qquad \text{or}
$$

$$
\hat{Z} = Z \cdot \left(\frac{(x - \hat{x}_0)\, n_x + (y - \hat{y}_0)\, n_y}{\left(x - x_0 + Z u_{\text{rot}_\epsilon}\right) n_x + \left(y - y_0 + Z v_{\text{rot}_\epsilon}\right) n_y - N Z}\right) \tag{3}
$$

From (3) we can see that $\hat{Z}$ is obtained from Z through multiplication by a factor given by the term inside the brackets, which we denote by D and call the distortion factor. In the forthcoming analysis we do not attempt to model the statistics of the noise and we will therefore ignore the noise term. Thus, the distortion factor takes the form

$$
D = \frac{(x - \hat{x}_0)\, n_x + (y - \hat{y}_0)\, n_y}{\left(x - x_0 + Z u_{\text{rot}_\epsilon}\right) n_x + \left(y - y_0 + Z v_{\text{rot}_\epsilon}\right) n_y} \tag{4}
$$

Equation (4) describes, for any fixed direction (n_x, n_y) and any fixed distortion factor D, a surface $f(x, y, Z) = 0$ in xyZ-space, which we call an iso-distortion surface. For specific values of the parameters $x_0, y_0, \hat{x}_0, \hat{y}_0, \alpha_\epsilon, \beta_\epsilon, \gamma_\epsilon$ and (n_x, n_y), this iso-distortion surface has the obvious property that points lying on it are distorted in depth by the same multiplicative factor D. The distortion of the estimated space can be studied by looking at these iso-distortion surfaces.

In order to derive the iso-distortion surfaces in 3D space (i.e., XYZ-space) instead of visual space (i.e., xyZ-space), we substitute $x = \frac{fX}{Z}$ and $y = \frac{fY}{Z}$ in (4), which gives the following equation:

$$
\begin{aligned}
&D((\alpha_\epsilon XY - \beta_\epsilon(X^2 + Z^2) + \gamma_\epsilon YZ)\, n_x \\
&\quad + (\alpha_\epsilon(Y^2 + Z^2) - \beta_\epsilon XY - \gamma_\epsilon XZ)\, n_y) \\
&\quad - \left(X - \frac{\hat{x}_0 Z}{f} - D\left(X - \frac{x_0 Z}{f}\right)\right) n_x \\
&\quad - \left(Y - \frac{\hat{y}_0 Z}{f} - D\left(Y - \frac{y_0 Z}{f}\right)\right) n_y = 0
\end{aligned} \tag{5}
$$

describing the iso-distortion surfaces as quadratic surfaces—in the general case, as hyperboloids. Figure 2 is obtained by the intersection of such surfaces with planes parallel to the X-Z plane, and looking at the resultant iso-distortion contours. We see that there are two common intersecting points of all the distortion contours in 3D space. At these intersecting points, the distortion factor is undefined. This phenomenon is related to the fundamental elements of the Cremona transformation and will be further elaborated upon in Sections 4 and 5.

The nature of such space distortion can be studied from two points of view. On the one hand, as mentioned previously, we can characterize the nature of space distortion in terms of the geometrical properties of the iso-distortion surfaces. This allows us (Cheong et al., 1998) to address several computational issues in

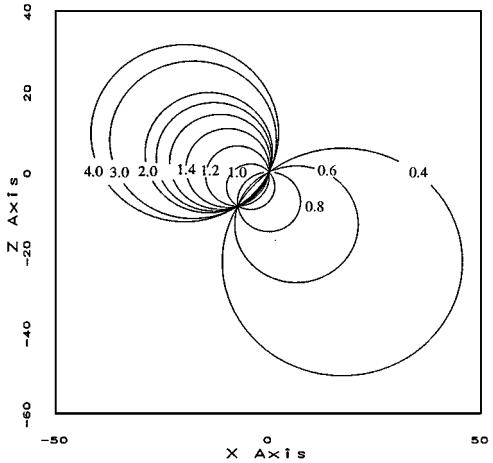

Figure 2. Iso-distortion contours in 3D space. $n_x = 1, n_y = 0$, $x_0 = 200$, $x_{0_\epsilon} = -100$, $\alpha_\epsilon = \gamma_\epsilon = 0$, and $\beta_\epsilon = -0.001$. Only the contours with $0.4 < D < 4$ are shown.

motion estimation:

- Efficacy of the visibility constraint
- Situations likely to give rise to ambiguities
- Anisotropy in the FOE uncertainty area (Duric and Aloimonos, 1994; Sinclair et al., 1994)
- Precision needed in an inertial sensor for accurate 3D motion estimation (the inertial sensor estimates rotation) (Viéville and Faugeras, 1989).

The geometry of such iso-distortion surfaces can also be used to explain various psychophysical phenomena in stereoscopic perception too, such as:

- Apparent Fronto Parallel Plane (AFPP)
- Apparent Distance Bisection (ADB)
- Distance Judgment from Motion and Stereo

For details, see (Fermüller et al., 1997). For a fuller description of the mathematical properties of the distorted stereoscopic space, see (Baratoff, 1997).

On the other hand, we can study the properties of the transformation itself, which we will show is a Cremona transformation. The rest of this paper (Sections 4–6) focus on studying the mathematical properties of the Cremona transformation, and then relating them back to the iso-distortion surfaces, thereby revealing further properties of the distorted space. In order to present these analyses visually, most of the investigation will be conducted by initially considering a particular gradient direction, say, $(n_x = 1, n_y = 0)$.

4. Cremona Space Transformation

A *Cremona transformation* $\phi : \mathcal{P}^d \to \hat{\mathcal{P}}^d$ is a transformation from a projective space to another of the same dimension. It has the property (*birationality*) that it is bijective almost everywhere except on the set of *F-elements* (abbreviation for *fundamental elements*) where ϕ becomes a one-to-many correspondence. The F-elements form a *variety* of $\mathcal{P}^d$ which by definition is the vanishing set of some homogeneous polynomials on $\mathcal{P}^d$.

We now introduce the homogeneous coordinates $[\mathcal{X}, \mathcal{Y}, \mathcal{Z}, \mathcal{W}]$, which are related to the non-homogeneous coordinates (X, Y, Z) by $(X, Y, Z) = [\mathcal{X}/\mathcal{W}, \mathcal{Y}/\mathcal{W}, \mathcal{Z}/\mathcal{W}, 1]$. Now define a Cremona transformation $\phi : \mathcal{P}^3 \to \hat{\mathcal{P}}^3$ (we think of $\mathcal{P}^3$ as the actual coordinates of the object but $\hat{\mathcal{P}}^3$ those of their estimated positions), where the image $[\hat{\mathcal{X}}, \hat{\mathcal{Y}}, \hat{\mathcal{Z}}, \hat{\mathcal{W}}]$ of a point $[\mathcal{X}, \mathcal{Y}, \mathcal{Z}, \mathcal{W}] \in \mathcal{P}^3$ is given by the formulae

$$[\hat{\mathcal{X}}, \hat{\mathcal{Y}}, \hat{\mathcal{Z}}, \hat{\mathcal{W}}] = [\phi_1, \phi_2, \phi_3, \phi_4] \tag{6}$$

Similarly, the inverse transformation $\phi^{-1} : \hat{\mathcal{P}}^3 \to \mathcal{P}^3$ is given by

$$[\mathcal{X}, \mathcal{Y}, \mathcal{Z}, \mathcal{W}] = [\hat{\phi}_1, \hat{\phi}_2, \hat{\phi}_3, \hat{\phi}_4] \tag{7}$$

The quantities ϕ_i are homogeneous polynomials (in $\mathcal{X}$, $\mathcal{Y}$, $\mathcal{Z}$ and $\mathcal{W}$) of degree n and $\hat{\phi}_i$ are homogeneous polynomials (in $\hat{\mathcal{X}}$, $\hat{\mathcal{Y}}$, $\hat{\mathcal{Z}}$ and $\hat{\mathcal{W}}$) of degree $\hat{n}$ ($\neq n$ in general). However, the transformation that we are going to study has the property $n = \hat{n} = 2$ and ϕ and ϕ^{-1} have similar expressions except for the parameters.

The F-elements of ϕ are precisely the common vanishing set (called a variety) of $\phi_i, 1 \leq i \leq 4$ where ϕ is indeterminate. However, it will be shown later that each point in the F-set in general corresponds to a positive dimensional variety in $\hat{\mathcal{P}}^d$ (called *a principal element*). Hence the F-set in $\mathcal{P}^d$ corresponds to some variety *P-set* (the union of all P-elements) in $\hat{\mathcal{P}}^d$.

In the case of $d = 3$, the F-elements can be points (simple or multiple) or curves. In particular, when $n = 2$, only three possibilities for $\hat{n} =$ degree of ϕ^{-1} and the F-set may occur:

a conic and a simple point	$\hat{n} = 2$
a line and three simple points	$\hat{n} = 3$
a double point and three simple points	$\hat{n} = 4$

(8)

For details, see (Hudson, 1927).

When $d = 3$, the set of all linear combinations of ϕ_i's form a three-dimensional (projective) family of surfaces S (defined by $c_1\phi_1 + c_2\phi_2 + c_3\phi_3 + c_4\phi_4 = 0$) (called *the homoloidal net spanned by* ϕ_i's). These are precisely the degree n surfaces that map to planes $c_1\hat{\mathcal{X}} + c_2\hat{\mathcal{Y}} + c_3\hat{\mathcal{Z}} + c_4\hat{\mathcal{W}} = 0$ in $\hat{\mathcal{P}}^3$. If a degree n surface S does not belong to the net spanned by ϕ_i's, its total image in $\hat{\mathcal{P}}^3$ is a degree $n\hat{n}$ surface (from (7)). This surface may contain P-elements if S contains any F-element, in which case the total image less all the P-elements, $\hat{S}$, is called the *proper homologue of* S.[1]

4.1. Singular Elements of Space Distortion Transformation

Consider the distortion factor given in Eq. (5). If we fix (n_x, n_y) to be in the horizontal direction, D can be

written as:

$$D = \frac{fX - \hat{x}_0 Z}{fX - x_0 Z + f(\alpha_\epsilon XY - \beta_\epsilon(X^2 + Z^2) + \gamma_\epsilon YZ)} \tag{9}$$

Since $\hat{X} = \frac{x\hat{Z}}{f} = D\frac{xZ}{f} = DX$, and similarly, $\hat{Y} = DY$, we can now express the space distortion in terms of the following homogeneous coordinates:

$$\begin{aligned}
\hat{\mathcal{X}} &= \phi_1 = (f\mathcal{X} - \hat{x}_0\mathcal{Z})\mathcal{X} \\
\hat{\mathcal{Y}} &= \phi_2 = (f\mathcal{X} - \hat{x}_0\mathcal{Z})\mathcal{Y} \\
\hat{\mathcal{Z}} &= \phi_3 = (f\mathcal{X} - \hat{x}_0\mathcal{Z})\mathcal{Z} \\
\hat{\mathcal{W}} &= \phi_4 = (f\mathcal{X} - x_0\mathcal{Z})\mathcal{W} + f(\alpha_\epsilon\mathcal{X}\mathcal{Y} \\
&\qquad - \beta_\epsilon(\mathcal{X}^2 + \mathcal{Z}^2) + \gamma_\epsilon\mathcal{Y}\mathcal{Z})
\end{aligned} \tag{10}$$

which is a Cremona space transformation of degree two. The transformation is uniquely defined except when all the (ϕ) vanish. This occurs when $(f\mathcal{X} - \hat{x}_0\mathcal{Z})$ and ϕ_4 both vanish. Substituting $\mathcal{X} = \frac{\hat{x}_0}{f}\mathcal{Z}$ into ϕ_4, we obtain:

$$\begin{aligned}
&\mathcal{Z}\big(-x_{0\epsilon} f\mathcal{W} + \alpha_\epsilon \hat{x}_0 f\mathcal{Y} - \beta_\epsilon \\
&\quad \times \big(\hat{x}_0^2 + f^2\big)\mathcal{Z} + \gamma_\epsilon f^2\mathcal{Y}\big) = 0
\end{aligned}$$

from which it can be concluded that the fundamental elements consist of two straight lines L_1 and L_2 given as follows:

$$\begin{aligned}
L_1 &= \{[\mathcal{X}, \mathcal{Y}, \mathcal{Z}, \mathcal{W}] \mid f\mathcal{X} - \hat{x}_0\mathcal{Z} = 0, \mathcal{Z} = 0\} \\
&= \{[0, \mathcal{Y}, 0, \mathcal{W}] \mid [\mathcal{Y}, \mathcal{W}] \in \mathcal{P}^1\} \\
L_2 &= \big\{[\mathcal{X}, \mathcal{Y}, \mathcal{Z}, \mathcal{W}] \mid f\mathcal{X} - \hat{x}_0\mathcal{Z} = 0, \\
&\qquad \big(-x_{0\epsilon} f\mathcal{W} + \alpha_\epsilon \hat{x}_0 f\mathcal{Y} - \beta_\epsilon\big(\hat{x}_0^2 + f^2\big)\mathcal{Z} \\
&\qquad + \gamma_\epsilon f^2\mathcal{Y}\big) = 0\big\} \\
&= \left\{\left[\frac{\hat{x}_0}{f}\mathcal{Z}, \frac{\beta_\epsilon\big(\hat{x}_0^2 + f^2\big)}{f(\alpha_\epsilon\hat{x}_0 + \gamma_\epsilon f)}\mathcal{Z} + \frac{x_{0\epsilon}}{\alpha_\epsilon\hat{x}_0 + \gamma_\epsilon f}\right.\right. \\
&\qquad \left.\left. \times \mathcal{W}, \mathcal{Z}, \mathcal{W}\right] \,\middle|\, [\mathcal{Z}, \mathcal{W}] \in \mathcal{P}^1\right\}
\end{aligned} \tag{11}$$

L_1 and L_2 intersect at the point $B, [0, \frac{x_{0\epsilon}}{\alpha_\epsilon\hat{x}_0 + \gamma_\epsilon f}, 0, 1]$ which constitutes the third fundamental element. B has multiplicity 2 (thus counted as two points) since it is the intersection of two lines. Thus the F-system is a degenerate conic (union of two lines) on which lies a double point B. It follows from (8) that the inverse transformation is also of degree two.

4.2. *Inverse Transformation*

We now derive the inverse transformation ϕ^{-1}:

$$\begin{aligned}
\phi^{-1}[\hat{\mathcal{X}}, \hat{\mathcal{Y}}, \hat{\mathcal{Z}}, \hat{\mathcal{W}}] &= [\mathcal{X}, \mathcal{Y}, \mathcal{Z}, \mathcal{W}] \\
&= \left[1, \frac{\mathcal{Y}}{\mathcal{X}}, \frac{\mathcal{Z}}{\mathcal{X}}, \frac{\mathcal{W}}{\mathcal{X}}\right] \\
&= \left[1, \frac{\hat{\mathcal{Y}}}{\hat{\mathcal{X}}}, \frac{\hat{\mathcal{Z}}}{\hat{\mathcal{X}}}, \frac{\mathcal{W}}{\mathcal{X}}\right]
\end{aligned} \tag{12}$$

$\frac{\hat{\mathcal{W}}}{\hat{\mathcal{X}}}$ is related to $\frac{\mathcal{W}}{\mathcal{X}}$ as follows:

$$\begin{aligned}
\frac{\hat{\mathcal{W}}}{\hat{\mathcal{X}}} &= \frac{(f\mathcal{X} - x_0\mathcal{Z})\mathcal{W} + f(\alpha_\epsilon\mathcal{X}\mathcal{Y} - \beta_\epsilon(\mathcal{X}^2 + \mathcal{Z}^2) + \gamma_\epsilon\mathcal{Y}\mathcal{Z})}{(f\mathcal{X} - \hat{x}_0\mathcal{Z})\mathcal{X}} \\
&= \frac{\mathcal{W}}{\mathcal{X}}\left(\frac{f - x_0\frac{\hat{\mathcal{Z}}}{\hat{\mathcal{X}}}}{f - \hat{x}_0\frac{\hat{\mathcal{Z}}}{\hat{\mathcal{X}}}}\right) + \frac{f\left(\alpha_\epsilon\frac{\hat{\mathcal{Y}}}{\hat{\mathcal{X}}} - \beta_\epsilon\left(1 + \left(\frac{\hat{\mathcal{Z}}}{\hat{\mathcal{X}}}\right)^2\right) + \gamma_\epsilon\frac{\hat{\mathcal{Y}}}{\hat{\mathcal{X}}}\frac{\hat{\mathcal{Z}}}{\hat{\mathcal{X}}}\right)}{f - \hat{x}_0\frac{\hat{\mathcal{Z}}}{\hat{\mathcal{X}}}}
\end{aligned}$$

Hence, $\frac{\mathcal{W}}{\mathcal{X}}$ can be expressed in terms of $\frac{\hat{\mathcal{W}}}{\hat{\mathcal{X}}}$ as follows:

$$\frac{\mathcal{W}}{\mathcal{X}} = \left[\frac{\hat{\mathcal{W}}\left(f - \hat{x}_0\frac{\hat{\mathcal{Z}}}{\hat{\mathcal{X}}}\right) - f\hat{\mathcal{X}}\left(\alpha_\epsilon\frac{\hat{\mathcal{Y}}}{\hat{\mathcal{X}}} - \beta_\epsilon\left(1 + \left(\frac{\hat{\mathcal{Z}}}{\hat{\mathcal{X}}}\right)^2\right) + \gamma_\epsilon\frac{\hat{\mathcal{Y}}}{\hat{\mathcal{X}}}\frac{\hat{\mathcal{Z}}}{\hat{\mathcal{X}}}\right)}{\hat{\mathcal{X}}\left(f - x_0\frac{\hat{\mathcal{Z}}}{\hat{\mathcal{X}}}\right)}\right]$$

Substituting the above relationship into (12), we obtain:

$$\begin{aligned}
\mathcal{X} &= (f\hat{\mathcal{X}} - x_0\hat{\mathcal{Z}})\hat{\mathcal{X}} \\
\mathcal{Y} &= (f\hat{\mathcal{X}} - x_0\hat{\mathcal{Z}})\hat{\mathcal{Y}} \\
\mathcal{Z} &= (f\hat{\mathcal{X}} - x_0\hat{\mathcal{Z}})\hat{\mathcal{Z}} \\
\mathcal{W} &= (f\hat{\mathcal{X}} - \hat{x}_0\hat{\mathcal{Z}})\hat{\mathcal{W}} - f(\alpha_\epsilon\hat{\mathcal{Y}}\hat{\mathcal{X}} \\
&\qquad - \beta_\epsilon(\hat{\mathcal{X}}^2 + \hat{\mathcal{Z}}^2) + \gamma_\epsilon\hat{\mathcal{Y}}\hat{\mathcal{Z}})
\end{aligned} \tag{13}$$

Hence, ϕ and ϕ^{-1} have similar expressions. Notice that the plane $f\hat{\mathcal{X}} - x_0\hat{\mathcal{Z}} = 0$ in $\hat{\mathcal{P}}^3$ is mapped onto a single point $[0, 0, 0, 1]$. *Hence the plane* $f\hat{\mathcal{X}} - x_0\hat{\mathcal{Z}} = 0$ *is a* P*-element.*

Carrying out the same operation as for ϕ, we obtain the fundamental elements of ϕ^{-1} as follows:

$$\begin{aligned}
&\hat{L}_1\colon [0, \hat{\mathcal{Y}}, 0, \hat{\mathcal{W}}] \\
&\hat{L}_2\colon \left[\frac{x_0}{f}\hat{\mathcal{Z}}, \frac{\beta_\epsilon\big(x_0^2 + f^2\big)}{f(\alpha_\epsilon x_0 + \gamma_\epsilon f)}\hat{\mathcal{Z}} + \frac{x_{0\epsilon}}{\alpha_\epsilon x_0 + \gamma_\epsilon f}\hat{\mathcal{W}}, \hat{\mathcal{Z}}, \hat{\mathcal{W}}\right] \\
&\hat{B}\colon \left[0, \frac{x_{0\epsilon}}{\alpha_\epsilon x_0 + \gamma_\epsilon f}, 0, 1\right]
\end{aligned} \tag{14}$$

4.3. Transformation of F-Lines

In general, a F-conic is transformed into a P-cone. In degenerate cases, where the conic becomes lines, the P-cone breaks up into planes. To see what these planes are, we need to lift the transformation $\phi : \mathcal{P}^3 \to \hat{\mathcal{P}}^3$ to another transformation $\tilde{\phi} : B_{L_i} \to \hat{\mathcal{P}}^3, i = 1, 2$. The variety B_{L_i} is the *blow-up* of $\mathcal{P}^3$ along L_i. It is isomorphic to $\mathcal{P}^3$ away from L_i but replaces L_i with $L_i \times \mathcal{P}^1$. We can think of the factor $\mathcal{P}^1$ as all the possible directions from which we can approach the line L_i. The reason for doing that is because points which are infinitesimally near L_i have well defined images in $\hat{\mathcal{P}}^3$ so that we can compute the "image" of L_i by taking the limit of the proper images of all possible directions of approach to L_i. See (Shafarevich, 1994) for details on blow-ups.

4.3.1. Transformation of L_1. We consider the blow-up of $\mathcal{R}^3_{X,Y,Z}$ (we look at the affine space in $\mathcal{P}^3$ defined by $\mathcal{W} \neq 0$) along L_1. Define the variety B_{L_1} as follows:

$$\begin{aligned} B_{L_1} &= \{((X, Y, Z), [s, t]) \mid Xt = Zs\} \\ &\subseteq \mathcal{R}^3_{X,Y,Z} \times \mathcal{P}^1_{s,t} \end{aligned}$$

There is a natural map $\pi : B_{L_1} \to L_1$ given by projection onto the first factor. We can regard $\nu = \frac{s}{t}$ as the direction of approach to L_1. For any point $p = (X, Y, Z)$ not on L_1, $X \neq 0$ or $Z \neq 0$, there is a unique point $\pi^{-1}(p) = ((X, Y, Z), [X, Z]) \in B_{L_1}$ over p. On the other hand, when p lies on L_1, $X = Z = 0$, $\pi^{-1}(p) = \mathcal{P}^1_{s,t}$. Hence the point $(0, Y, 0)$ on L_1 can be regarded as being replaced by a copy of $\mathcal{P}^1$ in B_{L_1}. Another interpretation of this copy of $\mathcal{P}^1$ is to recognize that L_1 is the projectivization of the two dimensional subspace $\boldsymbol{L}_1$ spanned by $\mathcal{Y}$ and $\mathcal{W}$. Then this copy of $\mathcal{P}^1$ is the projectivization of all the normal directions to L_1, $\mathcal{P}(\mathcal{R}^4/\boldsymbol{L}_1)$.

Using the relation $X = \nu Z$ on B_{L_1}, consider the lifting of $\phi, \tilde{\phi} : B_{L_1} \to \hat{\mathcal{P}}^3$:

$$\begin{aligned} &\tilde{\phi}\,((X, Y, Z), [s, t]) = \phi[\mathcal{X}, \mathcal{Y}, \mathcal{Z}, \mathcal{W}] \\ &= [\mathcal{X}(f\nu - \hat{x}_0), \mathcal{Y}(f\nu - \hat{x}_0), \mathcal{Z}(f\nu - \hat{x}_0), \\ &\quad \mathcal{W}(f\nu - x_0) + f\mathcal{Y}(\alpha_\epsilon \nu + \gamma_\epsilon) - f\beta_\epsilon(\mathcal{X}\nu + \mathcal{Z})] \end{aligned}$$

The image of the point $p = (0, Y_0, 0)$, $Y_0 = \mathcal{Y}_0/\mathcal{W}_0 = \omega$ on L_1 can be obtained by substituting $\mathcal{X} = 0$, $\mathcal{Z} = 0$ into the above equation:

$$\begin{aligned} &[0, \mathcal{Y}(f\nu - \hat{x}_0), 0, \mathcal{W}(f\nu - x_0) + f\mathcal{Y}(\alpha_\epsilon \nu + \gamma_\epsilon)] \\ &= \left[0, \frac{\omega(f\nu - \hat{x}_0)}{(f\nu - x_0) + f\omega(\alpha_\epsilon \nu + \gamma_\epsilon)}, 0, 1\right] \end{aligned} \tag{15}$$

which is the line $\hat{L}_1$ as defined in (14) as ν varies in $\mathcal{P}^1_{s,t}$. As ω varies, each point on L_1 gives rise to the same image $\hat{L}_1$. It is easy to verify that if we had performed the blow-up to the affine space defined by $\mathcal{Y} \neq 0$ along L_1, we would have found that the point at infinity, $[0, 1, 0, 0]$, on L_1 is mapped to $\hat{L}_1$ too:

$$\text{The image is } [0, (f\nu - \hat{x}_0), 0, f(\alpha_\epsilon \nu + \gamma_\epsilon)].$$

i.e., the limit of (15) as $\omega \to \infty$. Thus the image of $L_1 - [0, 0, 0, 1]$ is a degenerate plane, consisting of infinite copies of the line $\hat{L}_1$. But $[0, 0, 0, 1]$ in $\mathcal{P}^3$ corresponds to the plane $f\hat{\mathcal{X}} - x_0\hat{\mathcal{Z}} = 0$ in $\hat{\mathcal{P}}^3$. Hence the P-element corresponding to L_1 is the plane $f\hat{\mathcal{X}} - x_0\hat{\mathcal{Z}} = 0$.

4.3.2. Transformation of L_2. From Eqs. (11) L_2 can be written as:

$$\begin{aligned} \mathcal{X} &= \frac{\hat{x}_0}{f}\mathcal{Z} \\ \mathcal{Y} &= \lambda\mathcal{Z} + \mu\mathcal{W} \end{aligned}$$

where for ease of presentation, we have defined λ and μ as follows:

$$\begin{aligned} \lambda &= \frac{\beta_\epsilon(\hat{x}_0^2 + f^2)}{f(\alpha_\epsilon \hat{x}_0 + \gamma_\epsilon f)} \\ \mu &= \frac{x_{0\epsilon}}{\alpha_\epsilon \hat{x}_0 + \gamma_\epsilon f} \end{aligned} \tag{16}$$

A general point p on L_2 has the following homogeneous coordinates:

$$\begin{aligned} p &= [\mathcal{X}_0, \mathcal{Y}_0, \mathcal{Z}_0, \mathcal{W}_0] \\ &= \left[\frac{\hat{x}_0}{f}(\omega - \mu), \lambda\omega, \omega - \mu, \lambda\right] \\ &= \left[\frac{\hat{x}_0}{f}\frac{(\omega - \mu)}{\lambda}, \omega, \frac{(\omega - \mu)}{\lambda}, 1\right] \end{aligned} \tag{17}$$

In the case of L_1, the definition of B_{L_1} hinges on the fact that L_1 is characterized by $\mathcal{X} = \mathcal{Z} = 0$. To blow

up along L_2, we change coordinates so that L_2 is characterized by $\mathcal{X}' = \mathcal{Z}' = 0$ in some new homogeneous coordinates. Let our new projective coordinates be

$$\begin{aligned} \mathcal{X}' &= f\mathcal{X} - \hat{x}_0\mathcal{Z} \\ \mathcal{Y}' &= \mathcal{Y} \\ \mathcal{Z}' &= \mathcal{Y} - \lambda\mathcal{Z} - \mu\mathcal{W} \\ \mathcal{W}' &= \mathcal{W} \end{aligned} \tag{18}$$

or, equivalently:

$$\begin{aligned} \mathcal{X} &= \frac{\mathcal{X}'}{f} + \frac{\hat{x}_0}{f\lambda}(\mathcal{Y}' - \mathcal{Z}' - \mu\mathcal{W}') \\ \mathcal{Y} &= \mathcal{Y}' \\ \mathcal{Z} &= \frac{1}{\lambda}(\mathcal{Y}' - \mathcal{Z}' - \mu\mathcal{W}') \\ \mathcal{W} &= \mathcal{W}' \end{aligned} \tag{19}$$

Define the blow-up B_{L_2} (of the affine space given by $\mathcal{W} = \mathcal{W}' \neq 0$) along L_2 as before:

$$\begin{aligned} B_{L_2} &= \{((X', Y', Z'), [s, t]) \mid X't = Z's\} \\ &\subseteq \mathcal{R}^3_{X',Y',Z'} \times \mathcal{P}^1_{s,t} \end{aligned}$$

where $(X', Y', Z') = [\mathcal{X}'/\mathcal{W}', \mathcal{Y}'/\mathcal{W}', \mathcal{Z}'/\mathcal{W}', 1]$. To obtain $\tilde{\phi} : B_{L_2} \to \hat{\mathcal{P}}^3$ in terms of $\mathcal{X}', \mathcal{Y}', \mathcal{Z}', \mathcal{W}'$, we substitute (19) into (10) to obtain:

$$\begin{aligned} \hat{\mathcal{X}} &= \nu\mathcal{Z}'\left(\frac{\nu\mathcal{Z}'}{f} + \frac{\hat{x}_0}{f\lambda}(\mathcal{Y}' - \mathcal{Z}' - \mu\mathcal{W}')\right) \\ \hat{\mathcal{Y}} &= \nu\mathcal{Z}'\mathcal{Y}' \\ \hat{\mathcal{Z}} &= \frac{\nu\mathcal{Z}'}{\lambda}(\mathcal{Y}' - \mathcal{Z}' - \mu\mathcal{W}') \\ \hat{\mathcal{W}} &= (f\mathcal{X} - x_0\mathcal{Z})\mathcal{W} + f(\alpha_\epsilon\mathcal{X}\mathcal{Y} \\ &\quad - \beta_\epsilon(\mathcal{X}^2 + \mathcal{Z}^2) + \gamma_\epsilon\mathcal{Y}\mathcal{Z}) \end{aligned} \tag{20}$$

Using the fact that on L_2, $\mathcal{X} = \frac{\hat{x}_0}{f}\mathcal{Z}$, $\mathcal{X}' = 0$, $\mathcal{Z}' = 0$ and that $\mathcal{Y}' = \mathcal{Y}$, $\mathcal{W}' = \mathcal{W}$, we obtain the image $\hat{L}^{(p)}$ of a point $p = [\mathcal{X}_0, \mathcal{Y}_0, \mathcal{Z}_0, \mathcal{W}_0]$, where $Y_0 = \mathcal{Y}_0/\mathcal{W}_0 = \omega$, on L_2 as follows:

$$\begin{aligned} &\left[\nu\frac{\hat{x}_0}{f\lambda}(\mathcal{Y} - \mu\mathcal{W}), \nu\mathcal{Y}, \frac{\nu}{\lambda}(\mathcal{Y} - \mu\mathcal{W}),\right. \\ &\left.\frac{\alpha_\epsilon\hat{x}_0 + \gamma_\epsilon f}{\lambda}(\mathcal{Y} - \mu\mathcal{W})\right] \\ &= \left[\frac{\hat{x}_0}{f}b_\nu, \frac{\lambda\omega}{\omega - \mu}b_\nu, b_\nu, 1\right] \\ &= \frac{\lambda b_\nu}{\omega - \mu}\left(\frac{\hat{x}_0}{f}\frac{(\omega - \mu)}{\lambda}, \omega, \frac{(\omega - \mu)}{\lambda}\right) \end{aligned} \tag{21}$$

where $b_\nu = \frac{\nu}{\alpha_\epsilon\hat{x}_0 + \gamma_\epsilon f}$ depends only on the direction of approach to p (measured by ν). From the above formula, the image of p is a line lying in the plane $\hat{\Pi}$ given by $\hat{\mathcal{X}} = \frac{\hat{x}_0}{f}\hat{\mathcal{Z}}$ and passing through the origin. Different points on this line come from different directions of approach to p as ν varies. If we identify $\mathcal{P}^3$ and $\hat{\mathcal{P}}^3$, we can see from the last line and (17) that $\hat{L}^{(p)}$ is the line joining the origin and p.

That the point at infinity, $[\frac{\hat{x}_0}{f}, \lambda, 1, 0]$ on L_2 is also mapped to a line in the plane $\hat{\mathcal{X}} = \frac{\hat{x}_0}{f}\hat{\mathcal{Z}}$ can be easily verified.

The plane Π in $\mathcal{P}^3$ defined by $\mathcal{X} = \frac{\hat{x}_0}{f}\mathcal{Z}$ is spanned by the two lines L_1 and L_2. With the identification $\mathcal{P}^3 = \hat{\mathcal{P}}^3$, we conclude that:

(a) Every point except $[0, 0, 0, 1]$ on L_1 corresponds to $\hat{L}_1$, the $\hat{Y}$-axis in $\hat{\mathcal{P}}^3$ (from (15)).
(b) $[0, 0, 0, 1]$ corresponds to the P-plane in $\hat{\mathcal{P}}^3$ defined by $f\hat{\mathcal{X}} - x_0\hat{\mathcal{Z}} = 0$ (from (13)).
(c) Every point p on L_2 corresponds to a line $\hat{L}^{(p)}$ joining the origin and p, lying in the plane $\hat{\Pi}$ in $\hat{\mathcal{P}}^3$ defined by $\hat{\mathcal{X}} = \frac{\hat{x}_0}{f}\hat{\mathcal{Z}}$ (from (21)).

Also, it is not hard to see that $\hat{\Pi}$ is ruled by $\hat{L}^{(p)}$ as p runs through L_2 and that every point on $\Pi - (L_1 \cup L_2)$ is mapped onto $[0, 0, 0, 1] \in \hat{\mathcal{P}}^3$. Hence, we can further conclude that:

(d) The plane $\Pi = \hat{\Pi}$ is invariant under ϕ (but not pointwise or even linewise).

From (a)–(d), we conclude that the P-cone is the union of the two planes $f\hat{\mathcal{X}} - x_0\hat{\mathcal{Z}} = 0$ and $f\hat{\mathcal{X}} - \hat{x}_0\hat{\mathcal{Z}} = 0$, corresponding to L_1 (actually only one point $[0, 0, 0, 1]$ on it) and L_2 respectively.

4.4. *Transformation of Lines and Planes which Contain Only L_1 (or L_2)*

A general variety (i.e., it is not a F-element) of $\mathcal{P}^3$ is transformed by ϕ into another in $\hat{\mathcal{P}}^3$ of the same dimension.

By (7), a general surface S in $\mathcal{P}^3$, say, $g_r(\mathcal{X}, \mathcal{Y}, \mathcal{Z}, \mathcal{W})$, of degree r, is mapped to the surface $g_r(\hat{\phi}_1, \hat{\phi}_2, \hat{\phi}_3, \hat{\phi}_4)$ or say $\hat{g}_{\hat{r}}(\hat{\mathcal{X}}, \hat{\mathcal{Y}}, \hat{\mathcal{Z}}, \hat{\mathcal{W}})$, of degree $\hat{r} = \hat{n}r$. If S contains certain F-elements, then the homologue (given by $\hat{g} = 0$) splits into a union of principal surfaces, corresponding to the F-elements, and a residual surface $\hat{S}$, of degree $< \hat{n}r$, which is the proper homologue of S. For example, if g is a scalar

linear combination of $\phi_1, \phi_2, \phi_3, \phi_4$, then $\hat{S}$ reduces to a plane.

For a curve C in $\mathcal{P}^3$, its degree is defined to be the number of intersection points with a general plane. A general curve C of degree m is mapped to a curve $\hat{C}$ of degree nm—for if C meets a general plane in $\mathcal{P}^3$ in m points, it must meet a general n-dric S in the net spanned by ϕ_i's in mn points.[2] The image of the n-dric is a plane $\hat{\pi}$ which meets the total image of C in mn points. As in the case of surfaces, if C passes through any F-points, the total image splits into a set of P-elements, and a residual $\hat{C}$ of degree $<nm$, which is the proper homologue of C.

In our case, ϕ is specialized such that the F-conic breaks up into a pair of intersecting lines L_1 and L_2, and that the P-cone in $\hat{\mathcal{P}}^3$ breaks up into two planes: the planes $\hat{\mathcal{X}} = \frac{x_0}{f}\hat{\mathcal{Z}}$ and $\hat{\mathcal{X}} = \frac{\hat{x}_0}{f}\hat{\mathcal{Z}}$.

In general, if a surface S defined by $g = 0$ (of degree r) passes through L_1 but not L_2, then $g = \mathcal{X}\psi_1 + \mathcal{Z}\psi_2$ for some degree $(r-1)$ homogeneous polynomials ψ_1 and ψ_2. Using the inverse formula for ϕ^{-1}, we can see that the total image of S consists of the P-element given by $\hat{\mathcal{X}} - \frac{x_0}{f}\hat{\mathcal{Z}} = 0$ (due to $[0, 0, 0, 1]$) and the proper homologue of degree $2r - 1$. For instance, planes that pass through L_1 but not through L_2 will be preserved as planes.

We shall now study how planes passing through L_1 but not L_2 (or vice versa) are transformed by ϕ to planes by looking at how lines which intersect only one of them are transformed.

4.4.1. Image of a Line L Intersecting L_1 But Not L_2. Any line L which intersects L_1 at, say $p = [0, \omega, 0, 1] = (0, \omega, 0)$ lies in some plane π given by $t\mathcal{X} - s\mathcal{Z} = 0$ with $[s, t] \epsilon \mathcal{P}^1$. Let $\frac{s}{t} = \nu$. Note that $\nu \neq \frac{\hat{x}_0}{f}$ since otherwise L lies on the plane Π defined by $f\mathcal{X} - \hat{x_0}\mathcal{Z} = 0$ and will have $[0, 0, 0, 1]$ as its proper homologue (together with two P-elements $\hat{L}_1$ and $\hat{L}^{(p')}$ where $p' = L \cap L_2$). So L is given by:

$$[\nu\mathcal{Z}, \delta\mathcal{Z} + \omega\mathcal{W}, \mathcal{Z}, \mathcal{W}] \tag{22}$$

where δ measures the slope of L in the plane π. Since $f\mathcal{X} - \hat{x}_0\mathcal{Z} \neq 0$, $\frac{\hat{\mathcal{X}}}{\hat{\mathcal{Z}}} = \frac{\mathcal{X}}{\mathcal{Z}} = \nu \neq \frac{\hat{x}_0}{f}$. *Thus $\hat{L}$, the image of L, lies on the plane $\hat{\mathcal{X}} = \nu\hat{\mathcal{Z}}$.*

Substituting the inverse formulae (13) for $\mathcal{Y}$, $\mathcal{Z}$ and $\mathcal{W}$ into the relation $\mathcal{Y} = \delta\mathcal{Z} + \omega\mathcal{W}$, we obtain:

$$(f\hat{\mathcal{X}} - x_0\hat{\mathcal{Z}})\hat{\mathcal{Y}} = \delta(f\hat{\mathcal{X}} - x_0\hat{\mathcal{Z}})\hat{\mathcal{Z}} + \omega(f\hat{\mathcal{X}} - x_0\hat{\mathcal{Z}}) \times \hat{\mathcal{W}} - \omega f(\alpha_\epsilon\hat{\mathcal{Y}}\hat{\mathcal{X}} - \beta_\epsilon(\hat{\mathcal{X}}^2 + \hat{\mathcal{Z}}^2) + \gamma_\epsilon\hat{\mathcal{Y}}\hat{\mathcal{Z}})$$

Substituting $\hat{\mathcal{X}} = \nu\hat{\mathcal{Z}}$, we get

$$\hat{\mathcal{Z}}(\hat{\mathcal{Y}} - \hat{\delta}\hat{\mathcal{Z}} - \hat{\omega}\hat{\mathcal{W}}) = 0 \tag{23}$$

where $\hat{\delta}$ and $\hat{\omega}$ are respectively given by:

$$\begin{aligned} \hat{\delta} &= \frac{\delta(f\nu - x_0) + \omega f\beta_\epsilon(\nu^2 + 1)}{f\nu - x_0 + \omega f(\alpha_\epsilon\nu + \gamma_\epsilon)} \\ \hat{\omega} &= \frac{\omega(f\nu - \hat{x}_0)}{f\nu - x_0 + \omega f(\alpha_\epsilon\nu + \gamma_\epsilon)} \end{aligned} \tag{24}$$

Setting $\hat{\mathcal{Z}} = 0$ in (23) gives us the line $\hat{L}_1$ which is the P-element corresponding to $p = L \cap L_1$. The proper homologue of L is $\hat{L}$ defined by

$$\hat{\mathcal{X}} = \nu\hat{\mathcal{Z}}, \quad \hat{\mathcal{Y}} = \hat{\delta}\hat{\mathcal{Z}} + \hat{\omega}\hat{\mathcal{W}}$$

Clearly, the plane π is ruled by lines described by (22). Thus any plane π with equation $\mathcal{X} = \nu\mathcal{Z}$ (including $\nu = \hat{x}_0/f$ from the previous section), is invariant under ϕ. However, it is not line-wise invariant.

Note that $\hat{\delta}$, the slope of $\hat{L}$, is dependent on δ and ω, but $\hat{\omega}$ depends only on ν. $[0, \hat{\omega}, 0, 1]$ is the point where $\hat{L}$ intersects $\hat{L}_1$. That is, *where $\hat{L}$ intersects $\hat{L}_1$ depends only on ν = slope of the plane on which L lies*. This agrees with the formula (15) in the blow-up along L_1 when we computed the image of the point $p = [0, \omega, 0, 1]$ on L_1 by taking the limit as we approach p from the plane π defined by $\mathcal{X} = \nu\mathcal{Z}$.

For a line L which intersects L_1 at $[0, 1, 0, 0]$ at infinity, its image can be found by taking the limit of $\hat{L}$ as $\omega \to \infty$. The image of such a line is given by:

$$\begin{aligned} \hat{\mathcal{X}} &= \nu\hat{\mathcal{Z}} \\ \hat{\mathcal{Y}} &= \frac{\beta_\epsilon(\nu^2 + 1)}{(\alpha_\epsilon\nu + \gamma_\epsilon)}\hat{\mathcal{Z}} + \frac{(f\nu - \hat{x}_0)}{f(\alpha_\epsilon\nu + \gamma_\epsilon)}\hat{\mathcal{W}} \end{aligned}$$

Note that for lines with $\omega = 0$ (these correspond to lines of sight passing through the origin), $\hat{\omega} = 0$ and $\hat{\delta} = \delta$. That is, points along a line of sight L will remain as points along the same line of sight in the distorted space.

4.4.2. Image of a Line L Intersecting L_2 But Not L_1. From the opening remarks on the transform of a line containing a F-point in Section 4.4, we know that the homologue of a line L intersecting L_2 at p is a degree 2 curve with two components, the transform of p, $\hat{L}^{(p)}$ and the proper homologue $\hat{L}$, of L.

Suppose a line L intersects L_2 at a point p given by (17)

$$\begin{aligned} p &= [\mathcal{X}_0, \mathcal{Y}_0, \mathcal{Z}_0, \mathcal{W}_0] \\ &= \left[\frac{\hat{x}_0}{f}(\omega-\mu), \lambda\omega, \omega-\mu, \lambda\right] \\ &= \left[\frac{\hat{x}_0}{f}\frac{(\omega-\mu)}{\lambda}, \omega, \frac{(\omega-\mu)}{\lambda}, 1\right], \end{aligned}$$

then L lies in some plane π' given by

$$\begin{aligned} \mathcal{X}' &= \nu\mathcal{Z}' \\ \mathcal{Y}' &= \delta\mathcal{Z}' + \omega\mathcal{W}' \end{aligned} \tag{25}$$

for some $\nu \neq 0$ ($\nu = 0$ yields the plane $\mathcal{X}' = f\mathcal{X} - \hat{x}_0\mathcal{Z} = 0$ which passes through both L_1 and L_2), where the $\mathcal{X}', \mathcal{Y}', \mathcal{Z}', \mathcal{W}'$ system is defined in (18).

Note that there is a relation among ω, μ and λ from the fact that $\phi_4(p) = 0$:

$$\begin{aligned} (\hat{x}_0 - x_0)\left(\frac{\omega-\mu}{\lambda}\right) + f\big[\alpha_e\mathcal{X}_0\mathcal{Y}_0 \\ - \beta_e\big(\mathcal{X}_0^2 + \mathcal{Z}_0^2\big) + \gamma_e\mathcal{Y}_0\mathcal{Z}_0\big] = 0 \end{aligned} \tag{26}$$

In terms of the $\mathcal{X}$, $\mathcal{Y}$, $\mathcal{Z}$ and $\mathcal{W}$ coordinates, L is the intersection of two planes given by

$$f\mathcal{X} - \hat{x}_0\mathcal{Z} = \nu(\mathcal{Y} - \lambda\mathcal{Z} - \mu\mathcal{W}) \tag{27}$$

$$\mathcal{Y} = \delta(\mathcal{Y} - \lambda\mathcal{Z} - \mu\mathcal{W}) + \omega\mathcal{W} \tag{28}$$

$\mathcal{W}$ in (27) can be expressed in terms of $\mathcal{Y}$ and $\mathcal{Z}$ using (28). Hence, L can also be realized as the intersection of two planes P_1 and P_2 given by:

$$\begin{aligned} f(\omega-\mu\delta)\mathcal{X} + \nu(\mu-\omega)\mathcal{Y} \\ + [\lambda\omega\nu - (\omega-\mu\delta)\hat{x}_0]\mathcal{Z} = 0 : P_1 \\ (1-\delta)\mathcal{Y} + \delta\lambda\mathcal{Z} - (\omega-\delta\mu)\mathcal{W} = 0 : P_2 \end{aligned} \tag{29}$$

Substituting the inverse formulae (13) for $\mathcal{X}$, $\mathcal{Y}$, $\mathcal{Z}$ and $\mathcal{W}$ into (29), we obtain two image quadrics $\hat{Q}_1$ and $\hat{Q}_2$. The intersection $\hat{Q}_1 \cap \hat{Q}_2$ has degree $2 \times 2 = 4$ and contains the proper homologue $\hat{L}$ of L, $\hat{L}^{(p)}$ and another degree 2 curve which is not a component of the homologue of L (see below).

Substituting (13) into the equation of P_1, we have

$$\begin{aligned} (f\hat{\mathcal{X}} - x_0\hat{\mathcal{Z}})[f(\omega-\mu\delta)\hat{\mathcal{X}} + \nu(\mu-\omega)\hat{\mathcal{Y}} \\ + [\lambda\omega\nu - (\omega-\mu\delta)\hat{x}_0]\hat{\mathcal{Z}}] = 0 \end{aligned} \tag{30}$$

describing a quadric $\hat{Q}_1$ which is the union of two planes $\hat{R}_1 \cup \hat{R}_2$ where $\hat{R}_1$ is given by $f\hat{\mathcal{X}} - x_0\hat{\mathcal{Z}} = 0$.

Similarly, substitution of (13) into the equation of P_2 gives us the image quadric $\hat{Q}_2$ given by

$$\begin{aligned} (f\hat{\mathcal{X}} - \hat{x}_0\hat{\mathcal{Z}})\hat{\mathcal{W}} - (f\hat{\mathcal{X}} - x_0\hat{\mathcal{Z}}) \\ \times\left[\frac{1-\delta}{\omega-\delta\mu}\hat{\mathcal{Y}} + \frac{\delta\lambda}{\omega-\delta\mu}\hat{\mathcal{Z}}\right] \\ - f[\alpha_\epsilon\hat{\mathcal{Y}}\hat{\mathcal{X}} - \beta_\epsilon(\hat{\mathcal{X}}^2 + \hat{\mathcal{Z}}^2) + \gamma_\epsilon\hat{\mathcal{Y}}\hat{\mathcal{Z}}] = 0 \end{aligned} \tag{31}$$

The total homologue corresponding to L is only $(\hat{R}_2 \cap \hat{Q}_2)$ where:

$$\begin{aligned} \hat{Q}_1 \cap \hat{Q}_2 &= (\hat{R}_1 \cup \hat{R}_2) \cap \hat{Q}_2 \\ &= (\hat{R}_1 \cap \hat{Q}_2) \cup (\hat{R}_2 \cap \hat{Q}_2) \end{aligned}$$

because we know that $\hat{R}_1$ is a F-plane in $\hat{\mathcal{P}}^3$ which maps onto $[0, 0, 0, 1]$ in $\mathcal{P}^3$, the F-point which L does not pass through. In any case, it is easy to verify that $(\hat{R}_1 \cap \hat{Q}_2)$ is $\hat{L}_1 \cup \hat{L}_2$, the F-set in $\hat{\mathcal{P}}^3$.

For the intersection $\hat{R}_2 \cap \hat{Q}_2$, it is easy to verify that the line $\hat{L}^{(p)}$, the P-element corresponding to the intersection $p = L_2 \cap L$, lies in both $\hat{R}_2$ (this is trivial) and $\hat{Q}_2$ (needs (26)). Therefore, $\hat{R}_2 \cap \hat{Q}_2$ must be a union of two line $\hat{L}^{(p)} \cup \hat{L}$, the second of which is the proper homologue of L.

Note that if p specializes to the double point B (i.e., $\omega = \mu$) on both L_1 and L_2, $\hat{R}_2 \cap \hat{Q}_2$ becomes $\hat{L}^1 \cup \hat{L}$.

In algebraic terms, it means that if we set the second factor of (30) to zero and substitute into (31), we must get a reducible quadratic polynomial. From (30):

$$\hat{\mathcal{Y}} = \frac{f(\omega-\mu\delta)}{\nu(\omega-\mu)}\hat{\mathcal{X}} + \frac{\lambda\omega\nu - (\omega-\mu\delta)\hat{x}_0}{\nu(\omega-\mu)}\hat{\mathcal{Z}}$$

Substituting the above into (31), we obtain

$$\begin{aligned} \nu(\omega-\mu)(f\hat{\mathcal{X}} - \hat{x}_0\hat{\mathcal{Z}})\hat{\mathcal{W}} - (f\hat{\mathcal{X}} - x_0\hat{\mathcal{Z}}) \\ \times\{f(1-\delta)\hat{\mathcal{X}} + [\lambda\nu - \hat{x}_0(1-\delta)]\hat{\mathcal{Z}}\} \\ - f\{(\alpha_\epsilon\hat{\mathcal{X}} + \gamma_\epsilon\hat{\mathcal{Z}})[f(\omega-\mu\delta)\hat{\mathcal{X}} + (\lambda\omega\nu \\ - (\omega-\mu\delta)\hat{x}_0)\hat{\mathcal{Z}}] - \nu(\omega-\mu)\beta_\epsilon(\hat{\mathcal{X}}^2 + \hat{\mathcal{Z}}^2)\} = 0 \end{aligned}$$

which can be factorized as:

$$\begin{aligned} (f\hat{\mathcal{X}} - \hat{x}_0\hat{\mathcal{Z}})\Big(\nu(\omega-\mu)\hat{\mathcal{W}} + [\nu(\omega-\mu)\beta_\epsilon \\ - (\omega-\mu\delta)f\alpha_\epsilon - (1-\delta)f]\hat{\mathcal{X}} \end{aligned}$$

$$\times \left[\frac{\nu f[\omega\lambda\gamma_\epsilon - (\omega-\mu)\beta_\epsilon]}{\hat{x}_0} - f\gamma_\epsilon(\omega-\mu\delta) - \lambda\nu\frac{x_0}{\hat{x}_0} + (1-\delta)x_0 \right] \hat{\mathcal{Z}} \Big) = 0$$

The first factor corresponds to a plane whose intersection with $\hat{R}_2$ is $\hat{L}^{(p)}$; the second factor corresponds to a plane whose intersection with $\hat{R}_2$ is our required $\hat{L}$. That is, the proper homologue of L defined by:

$$\begin{aligned} & f(\omega-\mu\delta)\mathcal{X} + \nu(\mu-\omega)\mathcal{Y} \\ & \quad + [\lambda\omega\nu - (\omega-\mu\delta)\hat{x}_0]\mathcal{Z} = 0 \\ & \nu(\omega-\mu)\mathcal{W} - (1-\delta)f\mathcal{X} \\ & \quad + [(1-\delta)\hat{x}_0 - \nu\lambda]\mathcal{Z} = 0 \end{aligned}$$

(whereby we have expressed P_2 in a different way by eliminating $\mathcal{Y}$) is $\hat{L}$ defined by:

$$\begin{aligned} & f(\omega-\mu\delta)\hat{\mathcal{X}} + \nu(\mu-\omega)\hat{\mathcal{Y}} \\ & \quad + [\lambda\omega\nu - (\omega-\mu\delta)\hat{x}_0]\hat{\mathcal{Z}} = 0 \\ & \nu(\omega-\mu)\hat{\mathcal{W}} + [\nu(\omega-\mu)\beta_\epsilon - (\omega-\mu\delta) \\ & \quad \times f\alpha_\epsilon - (1-\delta)f]\hat{\mathcal{X}} \\ & \quad + \left[\frac{\nu f[\omega\lambda\gamma_\epsilon - (\omega-\mu)\beta_\epsilon]}{\hat{x}_0} - f\gamma_\epsilon(\omega-\mu\delta) \right. \\ & \qquad \left. - \lambda\nu\frac{x_0}{\hat{x}_0} + (1-\delta)x_0 \right] \hat{\mathcal{Z}} = 0 \end{aligned}$$

4.5. Forms of ϕ and ϕ^{-1}

The observed symmetry between ϕ and ϕ^{-1} is related to the fact that the projection center (0, 0, 0, 1) is part of the F-set, which results in the particularly simple form of ϕ:

$$\begin{aligned} \phi_1 &= (f\mathcal{X} - \hat{x}_0\mathcal{Z})\mathcal{X} \\ \phi_2 &= (f\mathcal{X} - \hat{x}_0\mathcal{Z})\mathcal{Y} \\ \phi_3 &= (f\mathcal{X} - \hat{x}_0\mathcal{Z})\mathcal{Z} \end{aligned}$$

or,

$$\hat{\mathcal{X}} : \hat{\mathcal{Y}} : \hat{\mathcal{Z}} = \mathcal{X} : \mathcal{Y} : \mathcal{Z} \qquad (32)$$

In this simple case, it can be shown that ϕ and ϕ^{-1} always have the same form (see Hudson, 1927, p. 184).

Thus, we can state the following: The P-elements in $\hat{\mathcal{P}}^3$ consist of the plane $f\hat{\mathcal{X}} - x_0\hat{\mathcal{Z}} = 0$ which corresponds to the point O (0, 0, 0, 1), and the P-cone (defined by the union of the two planes $f\hat{\mathcal{X}} - x_0\hat{\mathcal{Z}} = 0$ and $f\hat{\mathcal{X}} - \hat{x}_0\hat{\mathcal{Z}} = 0$) which corresponds to a conic defined by the union of the two lines L_1 and L_2. Similarly, the P-elements in $\mathcal{P}^3$ consist of the plane $f\mathcal{X} - \hat{x}_0\mathcal{Z} = 0$ which corresponds to the point $\hat{O}$ (0, 0, 0, 1), and the P-cone (defined by the union of the two planes $f\mathcal{X} - x_0\mathcal{Z} = 0$ and $f\mathcal{X} - \hat{x}_0\mathcal{Z} = 0$) which corresponds to a conic defined by the union of the two lines $\hat{L}_1$ and $\hat{L}_2$. Equation (32) also succinctly describes the result obtained in Section 4.4.1 that a ray of the star at O will map to the same ray of the star at $\hat{O}$. Visually, this means that the displacement of a point in 3D space caused by the distortion transformation is always in the direction of its line of sight. Indeed, the order of points along a line of sight can always be determined despite the distortion transformation (see Appendix A). Such ordinal depth information constitutes a less metrical way of representing depth than those traditionally used and has attracted much research interest recently (Garding et al., 1995, Todd and Reichel, 1989).

5. Revisiting Iso-Distortion Surfaces

Referring to Fig. 2, the two common intersecting points of all the iso-distortion contours are exactly the points where L_1 and L_2 intersect the X-Z plane. However, although all iso-distortion surfaces contain L_1 and L_2, they do not fall under the homoloidal net spanned by ϕ_i's, as we shall show now.

From the formula for the distortion factor D in (9), we can also write D as

$$D = \frac{(f\mathcal{X} - \hat{x}_0\mathcal{Z})\mathcal{W}}{(f\mathcal{X} - x_0\mathcal{Z})\mathcal{W} + f(\alpha_\epsilon\mathcal{X}\mathcal{Y} - \beta_\epsilon(\mathcal{X}^2 + \mathcal{Z}^2) + \gamma_\epsilon\mathcal{Y}\mathcal{Z})}$$

For convenience, we define ϕ_5 as $(f\mathcal{X} - \hat{x}_0\mathcal{Z})\mathcal{W}$. The D-iso-distortion surface, Q_D, is a quadric given by the equation $\phi_5 - D\phi_4 = 0$. However, D is indeterminate along a set where $\phi_4 = \phi_5 = 0$. Easy calculations show that this set is the union of $L_1 \cup L_2$ and a conic C at infinity defined by $\mathcal{W} = \alpha_\epsilon\mathcal{X}\mathcal{Y} - \beta_\epsilon(\mathcal{X}^2 + \mathcal{Z}^2) + \gamma_\epsilon\mathcal{Y}\mathcal{Z} = 0$.

Hence, *every iso-distortion surface passes through* $L_1 \cup L_2 \cup C$.

From the opening remarks in Section 4.4, the total homologue of the D-iso-distortion surface Q_D is the union of two planes $f\mathcal{X} - \hat{x}_0\mathcal{Z} = 0$ and $f\mathcal{X} - x_0\mathcal{Z} =$

0 (since Q_D contains the point [0, 0, 0, 1] and the line L_2 in $\mathcal{P}^3$), and a quadric $\hat{Q}_D$ which is the proper homologue. We can verify that easily by substituting the formulae of ϕ^{-1} into the equation of Q_D, obtaining:

$$\begin{aligned}(f\hat{\mathcal{X}} - \hat{x}_0\hat{\mathcal{Z}})(f\hat{\mathcal{X}} - x_0\hat{\mathcal{Z}})[(f\hat{\mathcal{X}} - \hat{x}_0\hat{\mathcal{Z}})\hat{\mathcal{W}} \\ - f[\alpha_\epsilon\hat{\mathcal{Y}}\hat{\mathcal{X}} - \beta_\epsilon(\hat{\mathcal{X}}^2 + \hat{\mathcal{Z}}^2) + \gamma_\epsilon\hat{\mathcal{Y}}\hat{\mathcal{Z}}] \\ -D(f\hat{\mathcal{X}} - x_0\hat{\mathcal{Z}})\hat{\mathcal{W}}] = 0\end{aligned}$$

Note that $\hat{Q}_D$ is precisely the $\frac{1}{D}$-iso-distortion surface of ϕ^{-1}.

Hence, we conclude that *the D-iso-distortion surface of ϕ transforms to the $\frac{1}{D}$-iso-distortion surface of ϕ^{-1}.*

6. Transformation of Surfaces Containing Both L_1 and L_2

We need some facts and theorems from commutative algebra in this section, namely, the Hilbert's Nullstellensatz and the relation between ideals in $\mathcal{C}[\mathcal{X}, \mathcal{Y}, \mathcal{Z}, \mathcal{W}]$ and varieties in $\mathcal{P}^3$. Appendix B summarizes some of the concepts from algebraic geometry required in this section.

Hilbert's Nullstellensatz is valid only over $\mathcal{C}$ or an algebraically closed field. We apply this result to obtain ideals and varieties over $\mathcal{C}$ and then notice that all of these are actually defined over $\mathcal{R}$.

Set F to be the union $L_1 \cup L_2$ for convenience. If a surface S in $\mathcal{P}^3$ contains F, then the *homogeneous ideal of S*, $I(S)$, is contained in the homogeneous ideal of F, $I(F)$. S is defined by a homogeneous polynomial g of degree r. g is in general a product of irreducible polynomials, possibly with repetitions. However, we can assume that g is an irreducible polynomial since the proper homologue of a reducible surface is the union of the proper homologues of its irreducible components (possibly with multiple components).

To determine the general form of g, we can make use of the fact that $I(S) \subset I(F)$. We compute both ideals first. Unfortunately, $I(F)$ is not necessarily $I = \langle\phi_1, \phi_2, \phi_3, \phi_4\rangle$, the ideal which yields F in the first place. This is the content of *Hilbert's Nullstellensatz*.

Hilbert's Nullstellensatz

Suppose a homogeneous ideal I in $\mathcal{C}[\mathcal{X}_1, \mathcal{X}_2, \ldots, \mathcal{X}_n]$ is generated by homogeneous polynomials $\phi_1, \phi_2, \ldots, \phi_s$ and the variety

$$\begin{aligned}V(I) = \{p \in \mathcal{P}^{n-1} \mid \phi_1(p) \\ = \phi_2(p) = \cdots = \phi_s(p) = 0\}\end{aligned}$$

is non-empty, then $I(V(I)) = \mathrm{Rad}(I)$.

In other words, if we start with an ideal I, look at $V(I)$ and then $I(V(I))$, we may end up getting polynomials $h \in \mathrm{Rad}(I) - I$ which do not originally belong to I (but some powers of h do) unless I is already a radical ideal. Also, it is possible to have two ideals $I_1 \neq I_2$ with $V(I_1) = V(I_2)$, but then $\mathrm{Rad}(I_1) = \mathrm{Rad}(I_2)$. Hence, there is a one-one correspondence between projective varieties and homogeneous radical ideals (excluding those irrelevant ideals, whose radical ideal is the maximal ideal $\langle\mathcal{X}_1, \mathcal{X}_2, \ldots, \mathcal{X}_n\rangle$, which yield the empty set).

It is easy to see that $I(S) = \langle g\rangle$ since g is irreducible. Now we see what the radical of $I_1 = \langle\phi_1, \phi_2, \phi_3, \phi_4\rangle$ is. Firstly, we observe that $V(I_1) = V(I_2)$ where $I_2 = \langle f\mathcal{X} - \hat{x}_0\mathcal{Z}, \phi_4\rangle$, i.e., $F = L_1 \cup L_2$ is presented as the intersection of a plane and a quadric. Hence, $\mathrm{Rad}(I_1) = \mathrm{Rad}(I_2)$. We make the following:

Claim: $\mathrm{Rad}(I_2) = I_2 = \langle f\mathcal{X} - \hat{x}_0\mathcal{Z}, \phi_4\rangle$

Proof: See Appendix B. □

Therefore, a degree r surface S containing F has its defining polynomial $g \in \langle f\mathcal{X} - \hat{x}_0\mathcal{Z}, \phi_4\rangle$ since $\langle g\rangle = I(S) \subset I(F) = I_2$, i.e.

$$g = (f\mathcal{X} - \hat{x}_0\mathcal{Z})\psi_1 + \phi_4\psi_2$$

for some degree $r-1$ homogeneous polynomial ψ_1 and degree $r-2$ homogeneous polynomial ψ_2.

The total homologue always contains the two planes defined by $f\hat{\mathcal{X}} - \hat{x}_0\hat{\mathcal{Z}} = 0$ and $f\hat{\mathcal{X}} - x_0\hat{\mathcal{Z}} = 0$ because S passes through L_1 and L_2. The proper homologue $\hat{S}$, is a degree $2r-2$ surface defined by $\hat{g}/(f\hat{\mathcal{X}} - \hat{x}_0\hat{\mathcal{Z}})(f\hat{\mathcal{X}} - x_0\hat{\mathcal{Z}})$, where $\hat{g}$ comes from substitution of the formulae of ϕ^{-1} into g.

The case $r = 2$ is particularly interesting since then ψ_1 is linear and ψ_2 is a constant. If ψ_1 does not have $\mathcal{W}$ as a summand, then $g = c_1\phi_1 + c_2\phi_2 + c_3\phi_3 + c_4\phi_4$, the proper homologue of S is a plane $c_1\hat{\mathcal{X}} + c_2\hat{\mathcal{Y}} + c_3\hat{\mathcal{Z}} + c_4\hat{\mathcal{W}} = 0$. If ψ_1 has $\mathcal{W}$ as a summand, then g is a linear combination of $\phi_1, \phi_2, \phi_3, \phi_4$ and ϕ_5. The proper homologue $\hat{S}$ is a quadric. The special case occurs when g is a linear combination of only ϕ_4 and ϕ_5, i.e., S is an iso-distortion surface.

7. Conclusions

Euclidean geometry has been used over the years by perceptual theorists to model perceptual space, that is, to represent physical space in the minds of seeing systems or in the computers controlling artificial vision systems. The major result of this paper is that no vision system can actually develop an Euclidean representation of its extra-personal space. Due to any slight errors in the estimation of its intrinsic or extrinsic parameters, the system can only estimate a distorted version of the physical space. In particular, a theory describing the distortion of the visual space due to errors in motion estimates has been developed. It represents a first step towards departing from the traditional Euclidean geometry used in the structure from motion problem. Specifically, it showed that the transformation between physical and perceptual space is a Cremona transformation. The systematic nature of the distortion is therefore made explicit by this transformation.

From a philosophical standpoint, this paper provides support for the empiricist viewpoint regarding the nature of our knowledge. In particular, to understand how the mind represents space, it is necessary to investigate scientifically the causal principles that in fact govern the mind's operation. The viewpoint emerging from this paper is that perceptual space appears to be governed by its own peculiar geometry whose understanding is a long-term research endeavour. This paper explored a few basic fundamentals of this geometry and opened up an exciting field of inquiry.

Specifically, we applied some established results from the mathematical literature on Cremona space transformation to the shape distortion transformation. We identified the fundamental elements of both the direct and the inverse transformation, and showed that they consist of degenerate conics and points. We also studied the transformation of space elements (lines, planes) that pass through these fundamental elements. Specifically, we derived planes that remain invariant under the distortion transformation. We also showed that points with the same gradient and lying on the same line of sight will remain as points along the same line of sight. Finally, we investigated the relationship between iso-distortion surfaces and the Cremona transformation ϕ.

There are several aspects of this work that could be further developed. First, the iso-distortion framework could be used to investigate properties of the visual space that remain invariant under distortions, due to imprecise motion estimates or imprecise estimates on the viewing geometry of a stereo configuration. Other important fields of inquiry include furthering the study of the mathematical properties of Cremona transformation and conducting a systematic psychophysical study on the effects of Cremona transformation on perceived visual space. Lastly, the distortion space of other departments of the Shape from X problems can be systematically worked out. When their respective laws of distortion, their individual weaknesses and strengths, and so forth, are understood, our representation of space will come to be securely grounded on a scientific foundation.

Appendix A

It is clear from Eq. (4) that the distorted depth $\hat{Z}$ given by DZ has the form $\frac{Z}{a+bZ}$, where a and b are given by:

$$\begin{aligned} a &= \frac{(x - x_0, y - y_0) \cdot \boldsymbol{n}}{(x - \hat{x}_0, y - \hat{y}_0) \cdot \boldsymbol{n}} \\ b &= \frac{\left(u_{\text{rot}_\epsilon}, v_{\text{rot}_\epsilon}\right) \cdot \boldsymbol{n}}{(x - \hat{x}_0, y - \hat{y}_0) \cdot \boldsymbol{n}} \end{aligned} \tag{33}$$

Since we are studying points lying along the same line of sight and with the same gradient $\boldsymbol{n}$, a and b are constant. Consider two such points, with depths Z_1 and Z_2 and their respective distortion factors denoted by D_1 and D_2. It can be easily shown that the sign of the depth difference $(Z_1 - Z_2)$ can be expressed as follows:

$$\text{sgn}(Z_1 - Z_2) = \text{sgn}(a D_1 D_2 (\hat{Z}_1 - \hat{Z}_2))$$

where we have used $\text{sgn}(\cdot)$ to denote the sign function. The signs of D_1, D_2, $\hat{Z}_1$ and $\hat{Z}_2$ are all known. Thus, if the sign of a is known, the relative ordering of Z_1 and Z_2 can always be determined. In particular, given the case where a is positive, only the following scenarios are possible:

1. if $D_1 > 0, D_2 > 0 \Rightarrow \text{sgn}(Z_1 - Z_2) = \text{sgn}(\hat{Z}_1 - \hat{Z}_2)$
2. if $D_1 < 0, D_2 < 0 \Rightarrow \text{sgn}(Z_1 - Z_2) = \text{sgn}(\hat{Z}_1 - \hat{Z}_2)$
3. if $D_1 D_2 < 0 \Rightarrow \text{sgn}(Z_1 - Z_2) = -\text{sgn}(\hat{Z}_1 - \hat{Z}_2)$ and the larger of the two depths will have a negative distortion factor.

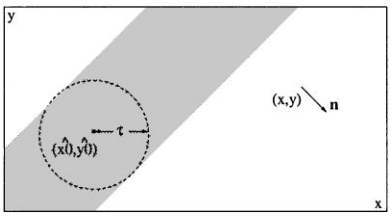

Figure 3. Unshaded area represents the region on the image plane where a is positive (for gradient direction $\boldsymbol{n}$).

The area where a is positive is determined readily if the uncertainty region of the FOE can be bounded by, say τ. This is illustrated in Fig. 3. Therefore if τ is sufficiently small, ordinal depth along a line of sight over much of the image region can be determined.

Appendix B

This appendix consists of a brief description of several notions in algebraic geometry that are used in this paper, chiefly in Section 6.

The solutions of a system of polynomial equations form a geometric object called a *variety*; the corresponding algebraic object is an *ideal*. There is a close relationship between ideals and varieties which reveals the intimate link between algebra and geometry. An excellent modern treatment of these topics is (Cox et al., 1992).

The ideals studied in algebraic geometry are subsets of the *polynomial ring* $k[x_1, \ldots, x_n]$, where $k[x_1, \ldots, x_n]$ denotes the set of all polynomials in $x_1, \ldots, x_n$ with coefficients in the algebraically closed *field* k. The polynomial ring used in this paper is $R = \mathcal{C}[\mathcal{X}, \mathcal{Y}, \mathcal{Z}, \mathcal{W}]$.

Definition. Let k be a field, and let $g_1, \ldots, g_s$ be polynomials in $k[x_1, \ldots, x_n]$. Then we set

$$V(g_1, \ldots, g_s) = \{(a_1, \ldots, a_n) \in k^n : g_i(a_1, \ldots, a_n) = 0 \text{ for all } 1 \le i \le s\}.$$

We call $V(g_1, \ldots, g_s)$ the *variety* defined by $g_1, \ldots, g_s$.[3]

Definition. A subset $I \subset k[x_1, \ldots, x_n]$ is an *ideal* if it satisfies:

(i) $0 \in I$.
(ii) If $g, h \in I$, then $g + h \in I$.
(iii) If $g \in I$ and $h \in k[x_1, \ldots, x_n]$, then $gh \in I$.

Definition. Let $h_1, \ldots, h_s$ be polynomials in $k[x_1, \ldots, x_n]$. Then we define

$$\langle h_1, \ldots, h_s \rangle = \left\{ \sum_{i=1}^{s} g_i h_i : g_1, \ldots, g_s \in k[x_1, \ldots, x_n] \right\}.$$

The crucial fact is $\langle h_1, \ldots, h_s \rangle$ is an ideal. An ideal $I = \langle h_1, \ldots, h_s \rangle$ is a *homogeneous ideal* when $h_1, \ldots, h_s$ are homogeneous polynomials.

A variety can be studied by passing to the ideal

$$I(V) = \{h \in k[x_1, \ldots, x_n] : h(x) = 0 \text{ for all } x \in V\}$$

of all polynomials vanishing on V. Conversely, given an ideal $I \subset k[x_1, \ldots, x_n]$, we can define the set

$$V(I) = \{x \in k^n : h(x) = 0 \text{ for all } h \in I\}$$

The following relationship exists between ideals and varieties:

Let V_1 and V_2 be varieties in k^n. Then:

(i) $V_1 \subset V_2$ if and only if $I(V_1) \supset I(V_2)$.
(ii) $V_1 = V_2$ if and only if $I(V_1) = I(V_2)$.

Though $I(V)$ and $V(I)$ give us a correspondence between ideals and varieties, the map $V(I)$ can fail to be one-to-one; different ideals can define the same variety. To establish an one-to-one correspondence, we need to introduce the notion of a *radical ideal*.

Definition. An ideal I is *radical* if $h^m \in I$ for any integer $m \ge 1$ implies that $h \in I$.

It is also useful to introduce the operation of taking the radical of an ideal.

Definition. Let $I \subset k[x_1, \ldots, x_n]$ be an ideal. The radical of I, denoted $\mathrm{Rad}(I)$, is the set

$$\{h : h^m \in I \text{ for some integer } m \ge 1\}.$$

$\mathrm{Rad}(I)$ clearly contains the ideal I (with $m = 1$).

Irreducible varieties arise in many context. Intuitively, a line or a plane are irreducible: they do not seem to be a union of finitely many simpler varieties. To caption this notion algebraically, we introduce the notion of *prime ideal*.

Definition. An ideal $I \in k[x_1, \ldots, x_n]$ is prime if whenever $g, h \in k[x_1, \ldots, x_n]$ and $g, h \in I$, then either $g \in I$ or $h \in I$.

A variety V irreducible if and only if $I(V)$ is a prime ideal. The simplest variety in k^n is a single point. The ideal I that corresponds to this point is said to be *maximal* because it has the property that any ideal J containing I is such that either $J = I$ or $J = k[x_1, \ldots, x_n]$.

Quotient Ring

We need to first introduce the notion of congruence modulo:

Definition. Let $I \subset R$ be an ideal, and let $g, h \in R$. We say g and h are congruent modulo I, if $g - h \in I$.

It can be shown that congruence modulo I is an equivalence relation on R. It partitions R into the equivalence classes of $[g]$, defined by

$$[g] = \{h \in R: g \text{ and } h \text{ are congruent modulo } I\}.$$

Given a ring R and an ideal $I \subset R$, the *quotient ring of R by I*, R/I, is defined to be the set of equivalence classes for congruence modulo I:

$$R/I = \{[g]: g \in R\}.$$

The sum and product operations *on classes* are defined by using the corresponding operations on elements of R. That is, $[g] + [h] = [g + h]$ and $[g][h] = [gh]$. It is easy to verify that R/I forms a ring with the above operations.

There is a simple but useful relation between prime ideals in R and prime ideals in R/I, namely, there is a one-one correspondence :

$$\text{prime ideals } A \subset R/I \leftrightarrow$$
$$\text{prime ideals } A' \subset R \text{ containing } I$$

Proof: We have the natural quotient map $\pi : R \to R/I$. Given a prime ideal $A \subset R/I$, $A' = \pi^{-1}(A)$ is clearly an ideal in R which contains I. To show that A' is a prime ideal, we need to show that if a product gh lies in A', then either $g \in A'$ or $h \in A'$. But if gh is in A', then $\pi(gh) = [gh] = [g][h]$ is in A. That means either $[g]$ or $[h]$ is in A since A is a prime ideal. Hence we can conclude that either $g \in \pi^{-1}[g] \subset A'$ or $h \in \pi^{-1}[h] \subset A'$.

On the other hand, if we have a prime ideal A' in R, $A = \pi(A')$ is easily shown to be an ideal in R/I. However, to show that A is prime, we need the fact that π is onto. Suppose $[gh] \in A$, we want to show that either $[g] \in A$ or $[h] \in A$. Since π is onto, there are $g', h' \in R$ such that $\pi(g') = [g]$ and $\pi(h') = [h]$. Clearly, $g'h' \in A'$ but A' is prime, therefore either $g' \in A'$ or $h' \in A'$. Applying π to both and we are done. □

Now we are already to compute the radical of I_1 with the following:

Claim: $\text{Rad}(I_2) = I_2 = \langle f\mathcal{X} - \hat{x}_0\mathcal{Z}, \phi_4\rangle$

Proof: There is an alternative but equivalent definition of the radical of an ideal I in R, namely, it is the intersection of all prime ideals in R containing I. With the above property of prime ideals in a quotient ring, it is sufficient to find all prime ideals in R/I, compute their intersection B, then we have $\text{Rad}(I) = \pi^{-1}(B)$ since π^{-1} respects intersections.

Hence, to find $\text{Rad}(I)$, it is sufficient to find all prime ideals in R/I, compute their intersection B, then $\text{Rad}(I) = \pi^{-1}(B)$.

Applying the above to our situation with $R = \mathcal{C}[\mathcal{X}, \mathcal{Y}, \mathcal{Z}, \mathcal{W}]$ and $I = I_2 = \langle f\mathcal{X} - \hat{x}_0\mathcal{Z}, \phi_4\rangle$, we find that

$$R/I_2 \equiv \mathcal{C}[\mathcal{Y}, \mathcal{Z}, \mathcal{W}]/\langle\overline{\phi_4}\rangle$$
$$= \mathcal{C}[\mathcal{Y}, \mathcal{Z}, \mathcal{W}]/\langle\mathcal{Z}(\mathcal{Y} - \lambda\mathcal{Z} - \mu\mathcal{W})\rangle$$

where $\overline{\phi_4}$ is ϕ_4 with the substitution $\mathcal{X} = \frac{\hat{x}_0}{f}\mathcal{Z}$.

From the view point of varieties, the substitution of $\mathcal{X} = \frac{\hat{x}_0}{f}\mathcal{Z}$ into ϕ_4 restricts our attention to the plane defined by $f\mathcal{X} - \hat{x}_0\mathcal{Z} = 0$ (now with homogeneous coordinates $\mathcal{Y}, \mathcal{Z}, \mathcal{W}$) in which lies two lines L_1 (defined by $\mathcal{Z} = 0$) and L_2 (defined by $\mathcal{Y} - \lambda\mathcal{Z} - \mu\mathcal{W} = 0$). See (16) for the definition of λ and μ.

The prime ideals in R/I_2 are in one-one correspondence with the (zero and one dimensional) irreducible varieties in $F = L_1 \cup L_2$, i.e., points on F and the lines L_1 and L_2 themselves. They are: the maximal ideals corresponding to points lying on L_1 and L_2, and two prime ideals $[\mathcal{Z}]$ (corresponding to L_1) and $[\mathcal{Y} - \lambda\mathcal{Z} - \mu\mathcal{W}]$ (corresponding to L_2), where $[\mathcal{Y}]$, $[\mathcal{Z}]$, and $[\mathcal{W}]$ are images of $\pi : R \to R/I_2$. However, the intersection of all the maximal ideals corresponding to points lying on L_1 all contain $[\mathcal{Z}]$ since

each of them does (similarly for points on L_2). Hence, it is sufficient to consider the intersection of the two prime ideals due to L_1 and L_2. It is $\mathrm{Rad}(R/I_2) = [\mathcal{Z}] \cap [\mathcal{Y} - \lambda\mathcal{Z} - \mu\mathcal{W}] = [\mathcal{Z}(\mathcal{Y} - \lambda\mathcal{Z} - \mu\mathcal{W})]$, which is the zero ideal in R/I_2. Therefore, pulling back to R, we have $\mathrm{Rad}(I_2) = I_2$. □

Notes

1. In the language of algebraic geometry, the homoloidal net of ϕ is called the *linear system* spanned by ϕ, the F-set of the net is called the *base locus* of the system, the P-set is called the *exceptional set*, the proper homologue is called the *proper transform.*
2. Such an n-dric is linearly equivalent to n copies of a general plane which meets C m times. Hence, by intersection theory, it meets C mn times.
3. Some writers use the term *algebraic subset* for the object as here defined, while reserving the term variety for the narrower meaning of *irreducible algebraic subset*.

References

Adiv, G. 1989. Inherent ambiguities in recovering 3D motion and structure from a noisy flow field. *IEEE Trans. Patt. Anal. Mach. Intell.*, 11:477–489.

Aloimonos, J., Weiss, I., and Bandopadhay, A. 1988. Active vision. *Int'l. J. of Computer Vision*, 2:333–356.

Baratoff, G. 1997. Distortion of stereoscopic visual space. Doctoral Dissertation, Center for Automation Research, University of Maryland, Technical Report CAR-TR-861.

Barron, J.L., Jepson, A.D., and Tsotsos, J.K. 1987. The sensitivity of motion and structure computations. In *Proc. 6th National Conf. on Artificial Intelligence*, Seattle, Washington, pp. 700–705.

Black, M. 1994. Recursive non-linear estimation of discontinuous flow fields. In *Proc. 3rd European Conf. on Computer Vision*, Stockholm, Sweden, pp. 138–145.

Bober, M. and Kittler, J. 1994. Robust motion analysis. In *Proc. IEEE Conf. on Computer Vision and Pattern Recognition*, Seattle, Washington, pp. 947–952.

Cheong, L.F., Fermüller, C., and Aloimonos, Y. 1998. Interaction between 3D shape and motion: Theory and applications. *Computer Vision and Image Understanding*, 71(3):356–372.

Cox, D., Little, J., and O'Shea, D. 1992. *Ideals, Varieties, and Algorithms: An Introduction to Computational Algebraic Geometry and Commutative Algebra.* Springer-Verlag: New York.

Daniilidis, K. and Nagel, H.-H. 1993. The coupling of rotation and translation in motion estimation of planar surfaces. In *Proc. IEEE Conf. on Computer Vision and Pattern Recognition*, New York City, New York, pp. 188–193.

Daniilidis, K. and Spetsakis, M.E. 1997. Understanding noise sensitivity in structure from motion. In *Visual Navigation: From Biological Systems to Unmanned Ground Vehicles*, Y. Aloimonos (Ed.), Lawrence Erlbaum Associates: New Jersey.

Duric, Z. and Aloimonos, Y. 1994. Estimating the heading direction using normal flow. *Int'l Journal of Computer Vision*, 13(1): 1–56.

Dutta, R. and Snyder, M.A. 1990. Robustness of correspondence-based structure from motion. In *Proc. Int. Conf. on Computer Vision*, Osaka, Japan, pp. 106–110.

Fermüller, C. 1995. Passive navigation as a pattern recognition problem. *Int. J. of Computer Vision*, 14:147–158.

Fermüller, C., Cheong, L.F., and Aloimonos, Y. 1997. Visual space distortion. *Biological Cybernetics*, 77:323–337.

Fleet, D. 1992. *Measurement of Image Velocity*. Kluwer Academic Publishers: Norwell.

Foley, J.M. 1967. Effects of voluntary eye movement and convergence on the binocular appreciation of depth. *Perception and Psychophysics*, 11:423–427.

Foley, J.M. 1980. Binocular distance perception. *Psychological Review*, 87(5):411–434.

Garding, J., Porrill, J., Mayhew, J.E.W., and Frisby, J.P. 1995. Stereopsis, vertical disparity and relief transformations. *Vision Research*, 35:703–722.

Heeger, D. and Jepson, A. 1992. Subspace methods for recovering rigid motion I: Algorithm and implementation. *Int'l J. of Computer Vision*, 7:95–117.

Heel, J. 1990. Direct estimation of structure and motion from multiple frames. M.I.T. Artif. Intell. Lab., M.I.T., AI Memo. 1190.

Horn, B.K.P. 1987. Motion fields are hardly ever ambiguous. *Int. J. of Computer Vision*, 1:259–274.

Hudson, H.P. 1927. *Cremona Transformations in Plane and Space.* The University Press: Cambridge. Also as 2nd edition, 1996.

Johnston, E.B. 1991. Systematic distortions of shape from stereopsis. *Vision Research*, 31:1351–1360.

Krames, J. 1940. Zur Ermittlung eines Objektes aus zwei perspektiven—Ein Beitrag zur Theorie der "gefährlichen örter". *Monatshefte für Mathematik und Physik*, 49:327–354.

Longuet-Higgins, H.C. 1981. A computer algorithm for reconstruction of a scene from two projections. *Nature*, 293:133–135.

Marr, D. 1982. *Vision.* Freeman: San Franscico.

Maybank, S. 1993. *Theory of Reconstruction from Image Motion.* Springer-Verlag: Berlin.

Negahdaripour, S. 1987. Ambiguities of a motion field. In *Proc. 1st Int. Conf. Computer Vision*, London, England, pp. 607–611.

Negahdaripour, S. 1989. Critical surface pairs and triplets. *Int. J. of Computer Vision*, 13:293–312.

Ogle, K.N. 1964. *Researches in Binocular Vision.* Hafner: New York.

Schunck, B.G. 1989. Image flow segmentation and estimation by constraint line clustering. *IEEE Trans. PAMI*, 11:1010–1027.

Semple, J. and Roth, L. 1949. *Introduction to Algebraic Geometry.* Oxford University Press: Oxford.

Shafarevich, I.R. 1994. *Basic Algebraic Geometry I.* Springer-Verlag: New York.

Sinclair, D., Blake, A., and Murray, D. 1994. Robust estimation of egomotion from normal flow. *Int. J. of Computer Vision*, 13:57–69.

Spetsakis, M.E. and Aloimonos, Y. 1988. Optimal computing of structure from motion using point correspondence. In *Proc. Int'l. Conf. on Computer Vision*, Tampa, Florida, pp. 449–453.

Thomas, J.I., Hanson, A., and Oliensis, J. 1993. Understanding noise: The critical role of motion error in scene reconstruction. In *Proc. DARPA Image Understanding Workshop*, Washington, DC, pp. 691–695.

Tittle, J.S., Todd, J.T., Perotti, V.J., and Norman, J.F. 1995. Systematic distortion of perceived three-dimensional structure from motion and binocular stereopsis. *J. of Experimental Psychology: Human Perception and Performance*, 21(3):663–678.

Todd, J.T. and Reichel, F.D. 1989. Ordinal structure in the visual perception and cognition of smoothly curved surfaces. *Psychological Review*, 96(4):643–657.

Tsai, R.Y. and Huang, T.S. 1984. Uniqueness and estimation of three-dimensional motion parameters of rigid objects with curved surfaces. *IEEE Trans. Patt. Anal. Mach. Intell.*, 6:13–27.

Uras, S., Girosi, F., and Torre, V. 1988. A computational approach to motion perception. *Biological Cybernetics*, 60:79–87.

Verri, A. and Poggio, T. 1989. Motion Field and Optical Flow: Qualitative Properties. *IEEE Trans. PAMI*, 11:490–498.

Viève, T. and Faugeras, O.D. 1989. Cooperation of the inertial and visual systems. In *Traditional and Non-Traditional Robotic Sensors*, T. Henderson (Ed.), Springer-Verlag: Berlin.

Weng, J., Huang, T.S., and Ahuja, N. 1991. *Motion and Structure from Image Sequences.* Springer-Verlag: New York.

Young, G.S. and Chellapa, R. 1992. Statistical analysis of inherent ambiguities in recovering 3D motion from a noisy flow field. *IEEE Trans. Patt. Anal. Mach. Intell.*, 14:995–1013.